

# THE LATENT VARIABLE PROXIMAL POINT ALGORITHM FOR VARIATIONAL PROBLEMS WITH INEQUALITY CONSTRAINTS

JØRGEN S. DOKKEN\*, PATRICK E. FARRELL†, BRENDAN KEITH‡, IOANNIS P. A. PAPADOPOULOS§, AND THOMAS M. SUROWIEC\*

**Abstract.** The latent variable proximal point (LVPP) algorithm is a framework for solving infinite-dimensional variational problems with pointwise inequality constraints. The algorithm is a saddle point reformulation of the Bregman proximal point algorithm. At the continuous level, the two formulations are equivalent, but the saddle point formulation is more amenable to discretization because it introduces a structure-preserving transformation between a latent function space and the feasible set. Working in this latent space is much more convenient for enforcing inequality constraints than the feasible set, as discretizations can employ general linear combinations of suitable basis functions, and nonlinear solvers can involve general additive updates. LVPP yields numerical methods with observed mesh-independence for obstacle problems, contact, fracture, plasticity, and others besides; in many cases, for the first time. The framework also extends to more complex constraints, providing means to enforce convexity in the Monge–Ampère equation and handling quasi-variational inequalities, where the underlying constraint depends implicitly on the unknown solution. In this paper, we describe the LVPP algorithm in a general form and apply it to twelve problems from across mathematics.

**1. Introduction.** Many problems in science, engineering, finance, and mathematics involve solving for a function subject to inequality constraints. Prominent examples include contact and damage in solid mechanics [86, 33], non-negativity of probability densities [113], invariant domain properties of hydrodynamic flow models [138], the pricing of American options [81], and the convexity condition on solutions to the Monge–Ampère equation [119]. While there are many popular methods for such problems, in general, it is quite difficult to achieve *mesh-independence*—that the number of iterations required for convergence of an optimization solver or Newton-type method does not grow unboundedly as the discretization is refined [4, 121, 135]—or *high-order accuracy*.

Where mesh-independent algorithms exist, they often return infeasible iterates [67, 86] or are tightly tied to lowest-order discretizations (e.g., piecewise linear finite elements), as they rely on monotonicity properties of the basis functions employed [37]. Typically, they also require parameters to pass to infinity for convergence [75, 78, 2]. While some methods have been proposed using high-degree basis approximations to construct feasible solutions (e.g., Bernstein polynomial-based discretizations [89] or biorthogonal bases [22]), these approaches are limited to pointwise bound constraints, and are generally mesh-dependent.

The first main challenge is the general lack of smoothness of many variational problems with inequality constraints. For example, the optimality conditions for the classical obstacle problem [88] are, in general, insufficiently regular to define a semismooth Newton method [74, 128, 129, 75] at the continuous level. This can seemingly be avoided on the finite-dimensional level by first discretizing the problem, where semismooth Newton methods are directly related to certain active set solvers

---

\*Department of Scientific Computing and Numerical Analysis, Simula Research Laboratory, Oslo, Norway ([dokken@simula.no](mailto:dokken@simula.no), [thomasms@simula.no](mailto:thomasms@simula.no))

†Mathematical Institute, University of Oxford, Oxford, United Kingdom and Mathematical Institute, Faculty of Mathematics and Physics, Charles University, Prague, Czechia ([patrick.farrell@maths.ox.ac.uk](mailto:patrick.farrell@maths.ox.ac.uk))

‡Division of Applied Mathematics, Brown University, Providence, RI, United States of America ([brendan\\_keith@brown.edu](mailto:brendan_keith@brown.edu))

§Weierstrass Institute, Berlin, Germany ([papadopoulos@wias-berlin.de](mailto:papadopoulos@wias-berlin.de))

for complementarity problems [102, 74]. However, the algorithm’s lack of validity at the continuous level manifests as mesh dependence [58, §4] as demonstrated in [Subsection 3.1](#) of this paper.

The second main challenge is that the feasible set  $K$ , implied by the underlying inequality constraint(s), is not a vector space; therefore, one cannot take arbitrary linear combinations of functions in  $K$  and remain in the set. Most successful discretization approaches approximate solutions using linear combinations of basis functions, but this strategy conflicts with the geometry imposed by the constraints. Moreover, most practical algorithms for solving optimization problems or nonlinear equations involve additive updates, which again conflicts.

In this paper, we introduce a general framework that adaptively regularizes variational problems with inequality constraints to overcome these challenges. The employed regularization permits  $K$  to be identified with a latent function space via smooth coordinate transformations arising from the set’s convex geometry. In turn, the framework enables the natural use of linear combinations of basis functions for approximation and additive update formulae. Furthermore, it results in regularized subproblems that are smooth enough to be solved with well-established mesh-independent techniques. We call this framework the *latent variable proximal point algorithm* (LVPP) and demonstrate some of its many potential applications by solving twelve challenging problems from across mathematics:

- The obstacle problem
- The Signorini problem
- Variational fracture
- Multi-phase gradient flow
- Quasi-variational inequalities
- Gradient constraints
- Eigenvalue constraints
- Intersections of constraints
- Constraining to the boundary of a set
- Linear equality constraints
- The eikonal equation
- The Monge–Ampère equation

The LVPP algorithm, which was first proposed by Keith and Surowiec in [85], is highly adaptable to various problem types, and possesses the following key properties, among others:

- (i) an infinite-dimensional formulation;
- (ii) observed mesh independence in both the mesh size and discretization degree;
- (iii) a simple mechanism for enforcing pointwise constraints on the discrete level without the need for a projection;
- (iv) ease of implementation — the algorithm reduces to repeatedly solving a system of smooth, nonlinear PDEs without requiring specialized discretizations, making it compatible with high-order methods and standard finite element libraries;
- (v) robust numerical performance, as convergence does not rely on any parameter passing to infinity.

No other framework satisfies all these properties simultaneously. For instance, penalty methods [75, 78, 2] satisfy (i), (ii), and (iv) but, without special care, often violate (iii) and (v), deliver infeasible solutions, and are known to be sub-optimal for high-order discretizations [69, §3.1]. Similarly, although multigrid methods [72, 79, 90] satisfy (iii) and (v), they are mildly mesh dependent, tied to low-order discretizations, and the implementation may be delicate for general problems.

In [Section 2](#), we describe the theoretical foundations of the LVPP algorithm. [Section 3](#) is dedicated to applying LVPP to pointwise bound constraints and includes example applications for the obstacle problem, contact mechanics, variational fracture, multiphase free boundary problems, and obstacle-type quasi-variational inequalities. [Section 4](#) focuses on more complicated convex constraints, such as norm and eigenvalue

constraints, as well as how to handle multiple simultaneous inequality constraints. [Section 5](#) demonstrates two ways to extend LVPP to equality constraints by first exploring the (non-convex) norm constraint  $|u| = 1$  and then analyzing general linear equality constraints, where we find that LVPP reduces to the well-known (linear) saddle-point formulation [\[32\]](#). Finally, in [Section 6](#), we describe applications to solving fully-nonlinear first- and second-order PDEs, using the eikonal and Monge–Ampère equations as examples. Our findings are summarized in [Section 7](#).

**2. Theoretical foundations.** We formally derive the general LVPP algorithm, drawing together classical notions from convex analysis and optimization, such as Legendre functions and the Bregman proximal point method. The section closes with a brief discussion of proximal numerical methods derivable from LVPP, including the proximal Galerkin method [\[85\]](#). It is important to note that while the majority of statements made in this section are rigorous, several key steps leading to the *general* form of LVPP have only been proven to date for bound constraints, see [\[85, Appendix A\]](#).

We choose to focus on variational problems posed on Lipschitz domains  $\Omega \subset \mathbb{R}^n$  with feasible sets  $K$  of the following form:

$$(2.1) \quad K = \{v \in V \mid Bv(x) \in C(x) \text{ for almost every } x \in \Omega_d \subset \overline{\Omega}\}.$$

Here,  $\Omega_d$  is a subset of the closure of  $\Omega$ ,  $V \subset L^1(\Omega)$  is a Banach space on  $\Omega$ , and  $B: V \rightarrow L^1(\Omega_d)$  is a bounded linear operator on  $V$  whose arguments in [\(2.1\)](#) are constrained to map pointwise a.e. in  $\Omega_d$  into a convex set  $C(x) \subset \mathbb{R}^m$ . Generally speaking,  $\Omega_d$  should be Hausdorff-measurable, with Hausdorff dimension  $d$  not necessarily equal to  $n$ . For example, in contact problems, we may wish to take  $\Omega_d \subset \partial\Omega$ , where  $d = n - 1$ . Moreover,  $C$  may vary from point to point, as in an obstacle problem, where  $B = \text{id}$  is the identity operator and  $\Omega_d = \Omega$ , specified functions give the upper and lower bounds on every  $v \in K$ . We refer to  $C = C(x)$  as the (pointwise) *feasible image* of  $B$ .

**2.1. Legendre functions.** The geometry of a closed convex set  $C \subset \mathbb{R}^m$  with a non-empty interior,  $\text{int } C \neq \emptyset$ , can be encoded into a *Legendre function*  $R: \mathbb{R}^m \rightarrow \mathbb{R} \cup \{+\infty\}$ . Introduced by Rockafellar in 1967 [\[115\]](#), see also [\[116, Chap. 26\]](#), Legendre functions constitute a special class of proper convex functions whose gradients  $\nabla R$  become singular on the boundary of their essential domains,  $\text{dom } R := \{a \in \mathbb{R}^m \mid R(a) < \infty\}$ . We denote by  $R^*(a^*) := \sup\{a \cdot a^* - R(a) \mid a \in \mathbb{R}^m\}$  the convex conjugate of  $R$ .

**THEOREM 2.1** (Rockafellar [\[115, Thm. 1\]](#)). *A proper convex function  $R$  is a Legendre function if and only if its convex conjugate  $R^*$  is also a Legendre function. Moreover,  $\nabla R: \text{int}(\text{dom } R) \rightarrow \text{int}(\text{dom } R^*)$  is a topological isomorphism with  $(\nabla R)^{-1} = \nabla R^*$ .*

From now on, we assume that  $R(a)/|a| \rightarrow +\infty$  as  $|a| \rightarrow \infty$  and  $\text{dom } R = C$ . The first property is equivalent to  $\text{dom } R^* = \mathbb{R}^m$  [\[25, Proposition 2.16\]](#), and so [Theorem 2.1](#) ensures that the gradient  $\nabla R$  is an isomorphism between  $\text{int } C$  and  $\mathbb{R}^m$ . Geometrically, this map defines geodesics in  $C$  that appear as straight lines in  $\mathbb{R}^m$  [\[9\]](#); see [Figure 1](#) for a depiction. As explained below, the inverse of the gradient of  $R$ , namely,  $\nabla R^*: \mathbb{R}^m \rightarrow \text{int } C$ , exposes a latent vector space enabling feasible and conforming discretizations of a wide variety of variational problems with inequality constraints.

The Legendre function  $R$  induces a non-symmetric notion of (squared) distance

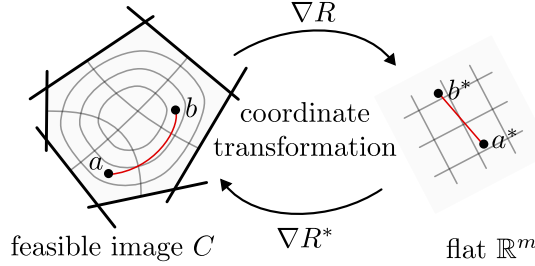


Fig. 1: The gradient of the Legendre function  $R$  is an isomorphism between the interior of the feasible image of an operator  $B$ , denoted  $\text{int } C$ , and  $\mathbb{R}^m$ . Here, curved geodesics in  $C$  are transformed into straight lines in  $\mathbb{R}^m$  [9]. The grey lines in the illustration depict the different coordinate systems on the two manifolds, while the red lines represent dual geodesics between points  $a$  and  $b$  in  $C$  and  $a^* := \nabla R(a)$  and  $b^* := \nabla R(b)$  in  $\mathbb{R}^m$ .

within the feasible image  $C$  via the concept of a Bregman divergence [34]:

$$(2.2) \quad D_R(a, b) := R(a) - R(b) - \nabla R(b) \cdot (a - b), \quad a \in C, b \in \text{int } C,$$

which measures the error in the first-order Taylor expansion of  $R$  over  $C$ . In turn, (2.2) induces a notion of distance in the feasible set  $K$ , given by  $\int_{\Omega_d} D_R(Bu, Bv) d\mathcal{H}_d$ , where  $d\mathcal{H}_d$  denotes the  $d$ -dimensional Hausdorff measure on  $\Omega_d$ . In this work, we only consider the settings  $\Omega_d = \Omega$  and  $\Omega_d \subset \partial\Omega$ , in which case  $d\mathcal{H}_d = d\mathcal{H}_n$  and  $d\mathcal{H}_d = d\mathcal{H}_{n-1}$  coincide with the standard Lebesgue volume and surface measures, respectively.

**2.2. The latent variable proximal point algorithm.** The Bregman divergence induced by a Legendre function has a regularizing effect on constrained optimization problems of the form

$$(2.3) \quad \min_{u \in K} J(u),$$

that is exploited in the *Bregman proximal point algorithm* [126]: for a suitable initial guess  $u^0 \in V$  and given a positive sequence of proximity parameters  $\{\alpha_k\}$ , compute

$$(2.4) \quad u^k \in \arg \min_{u \in K} J(u) + \alpha_k^{-1} \int_{\Omega_d} D_R(Bu, Bu^{k-1}) d\mathcal{H}_d, \quad k = 1, 2, \dots$$

This algorithm adaptively regularizes (2.3), with the striking property that it converges arbitrarily quickly for convex  $J$ :

$$(2.5) \quad J(u^k) - J(u^*) \leq \left( \sum_{i=1}^k \alpha_i \right)^{-1} \int_{\Omega_d} D_R(Bu^*, Bu^0) d\mathcal{H}_d,$$

where  $u^*$  is any minimizer of  $J$  in  $K$  [42]. If  $J$  is strongly convex, then  $u^*$  is unique, and we obtain strong convergence of  $u^k \rightarrow u^*$  in  $V$ . Since  $\alpha_k$  does not need to go to infinity for convergence, the algorithm can be very robust; the algorithm can also be very fast if the sequence grows rapidly. In addition to convex problems, we also consider non-convex functionals (Subsection 3.3), quasi-variational inequalities (Subsection 3.5), and non-convex feasible sets (Subsection 5.1) in this work.

Solving (2.4) generally requires gradient-based methods and thus, differentiability of the Bregman divergence. To this end, the singularity of  $\nabla R$  on  $\partial C$  leads us to a condition familiar to interior point methods:  $Bu^k(x) \in \text{int } C(x)$  for a.e. point  $x \in \Omega_d$ . For bound constraints, this inclusion is even uniformly satisfied, see [85]. In turn, each perturbed subproblem (2.4) will have first-order optimality conditions that are smooth *equations*, in contrast to, for instance, quadratic penalty or augmented Lagrangian methods, which naturally include nonsmooth operators. Thus, the first order optimality conditions for (2.4), amount to

$$(2.6) \quad \text{find } u^k \in K : \quad \alpha_k J'(u^k) + B^* \nabla R(Bu^k) - B^* \nabla R(Bu^{k-1}) = 0,$$

where  $J'$  is the Fréchet derivative of  $J$  and  $B^*$  is the dual (conjugate) operator of  $B$ ; cf. the derivation of the *entropic Poisson equation* in [85].

While the Bregman proximal point algorithm is theoretically attractive, its practical implementation (2.6) requires discretizing functions  $u^k$  in the feasible set  $K$ . The key novelty of the *latent variable proximal point (LVPP) algorithm* is to rewrite the Bregman proximal point algorithm (2.4) as a sequence of saddle point problems: starting from some  $\psi^0 \in W$ , find  $(u^k, \psi^k) \in V \times W$  satisfying

$$(2.7a) \quad \alpha_k J'(u^k) + B^* \psi^k = B^* \psi^{k-1},$$

$$(2.7b) \quad Bu^k - \nabla R^*(\psi^k) = 0,$$

for  $k = 1, 2, \dots$ , where  $\psi^k := \nabla R(Bu^k)$  is a *latent variable* lying in a suitable Banach space  $W$  over which  $\nabla R^*: W \rightarrow B(K)$  is well-defined and continuously invertible onto its range. In this paper, we adopt the simplifying conventions  $\psi^0 = 0$  and  $W = L^\infty(\Omega_d)$ . However, the identity  $W = L^\infty(\Omega_d)$  can only be guaranteed by technical regularity conditions that are outside the scope of this work; cf. [85]. In general, problems (2.4) and (2.7) are equivalent in that  $u^k$  coincide for each iteration  $k$ . However, the saddle point formulation (2.7) yields two approximations to the pointwise observable  $Bu$ ; namely,  $Bu^k$  and  $\nabla R^*(\psi^k)$ , which differ from each other after discretization. Since convergence of the algorithm is proven at the infinite-dimensional level, one can generically hope for mesh-independent convergence of its discretizations.

The saddle point reformulation (2.7) has at least four major advantages. First, *this formulation does not require discretizing the feasible set  $K$* . Instead, it only requires discretizing the vector spaces  $V \supset K$  and  $W$ . Thus, LVPP removes any need for special discretizations, e.g., positive basis functions, enabling the use of convenient and familiar discretizations with well-understood approximation properties, e.g., *hp*-FEM [108] and high-degree spectral approximations for the obstacle problem (cf. Subsection 3.1). Second, LVPP is guaranteed to return discretized iterates in  $K$ . Indeed, although the approximate observable  $Bu_h^k$  may not belong to  $K$  after discretizing (2.7), the second approximation  $\nabla R^*(\psi_h^k)$  always does by construction (recall  $\nabla R^*: \mathbb{R}^m \rightarrow \text{int } C$ ). Third, the subproblems (2.7) are often smoother than those arising in other algorithms and can be solved by standard Newton methods. Finally, because of this smoothness, the number of required iterations is typically bounded as the resolution of the discretization increases.

LVPP was first introduced in the context of pointwise bound constraints ( $B = \text{id}$ ,  $\Omega_d = \Omega$ ) [85]. In this work, we make several major extensions, allowing us to systematically tackle a wide variety of variational problems with gradient ( $B = \nabla$ ,  $\Omega_d = \Omega$ ), Hessian ( $B = \nabla^2$ ,  $\Omega_d = \Omega$ ), and trace constraints ( $B = \gamma$ ,  $\Omega_d = \partial\Omega$ ), where

Feasible set $K$	Legendre function $R$	$B$	$\nabla R^*(\psi)$
$\{u \geq \phi\}$	$(a - \phi) \ln(a - \phi) - (a - \phi)$	id	$\phi + \exp \psi$
$\{\phi_1 \leq u \leq \phi_2\}$	$(a - \phi_1) \ln(a - \phi_1) + (\phi_2 - a) \ln(\phi_2 - a)$	id	$\frac{\phi_1 + \phi_2 \exp \psi}{1 + \exp \psi}$
$\{\gamma u \geq 0\}$	$a \ln a - a$	$\gamma$	$\exp \psi$
$\{(\gamma u) \cdot n \geq 0\}$	$a \ln a - a$	$\gamma(\cdot) \cdot n$	$\exp \psi$
$\{ \nabla u  \leq \phi\}$	$-\sqrt{\phi^2 -  a ^2}$	$\nabla$	$\frac{\phi \psi}{\sqrt{1 +  \psi ^2}}$
$\{u \geq 0, \sum_i u_i = 1\}$	$\sum_i a_i \ln(a_i)$	id	$\frac{\exp \psi}{\sum_i \exp \psi_i}$
$\{\det(\nabla^2 u) \geq 0\}$	$\text{tr}(a \ln a - a)$	$\nabla^2$	$\exp \psi$

Table 1: Some examples of the feasible set (2.1) with an associated Legendre function  $R$ . Note that the Legendre function choices are not unique, and many are often available for the same feasible set  $K$ . Here,  $n$  is the unit outward normal to  $\partial\Omega$ , id is the identity operator,  $\gamma$  is the trace operator, and  $\nabla^2$  is the Hessian operator. The function  $u$  can be scalar- or vector-valued, as appropriate. Likewise, exp denotes the scalar, component-wise, or matrix exponential function.

$\gamma$  is the trace operator. See Table 1 for a partial list. As a general principle, we choose  $R$  so that  $\nabla R^*$  is Fréchet differentiable. For example, in our treatment of the obstacle problem presented in Subsection 3.1, we consider taking  $R(a) = (a - \phi) \ln(a - \phi) - (a - \phi)$ , leading to the exponential map  $\nabla R^*(\psi^k) = \phi + \exp \psi^k$  in (2.7), which is infinitely Fréchet differentiable on  $W = L^\infty(\Omega)$ . This particular setting was investigated in detail in [85]. However, we note that the choice of the Legendre function is flexible in LVPP, and often, many appealing choices can be found for solving the same problem.

**2.3. Proximal Galerkin and other proximal numerical methods.** To date, the LVPP algorithm has mainly been used as a means of deriving proximal Galerkin finite element methods [85, 62, 108], which arise from Galerkin discretizations of the LVPP saddle point problems (2.7) using conforming finite element spaces. However, since LVPP is derived at the continuous level, it is agnostic to the method of discretization. Therefore, *LVPP should be seen as a framework for deriving numerical methods rather than a numerical method itself*. We highlight this perspective in Subsection 3.1 below by introducing other proximal numerical methods in addition to proximal Galerkin. Nevertheless, the majority of methods in this work are proximal Galerkin methods.

No exotic elements are needed for the finite element methods in this paper. Although finite element discretizations of saddle-point problems can come in many forms, with different properties depending on chosen bases or subspaces, we choose to focus on elements discretizing the  $L^2$  de Rham complex (continuous Lagrange etc.) [15]. These elements are widely available in free software, meaning that every derived method should be implementable by non-experts.

**3. Pointwise bound constraints.** We begin our study of LVPP with pointwise bound constraints. This is the simplest and best-understood class of problems,

allowing us to compare the performance of the derived methods to other standard approaches in the literature.

**3.1. Example 1: The obstacle problem.** We first consider the (unilateral) obstacle problem: minimize the Dirichlet energy

$$(3.1) \quad J(u) = \frac{1}{2} \int_{\Omega} \nabla u \cdot \nabla u \, dx - \int_{\Omega} f u \, dx,$$

where  $f \in L^2(\Omega)$  is a prescribed body force, over the feasible set

$$(3.2) \quad K = \{v \in H_0^1(\Omega) \mid v \geq \phi_1 \text{ a.e. in } \Omega\},$$

which is obtained from the general feasible set (2.1) by choosing  $V = H_0^1(\Omega)$ ,  $B = \text{id}$ ,  $\Omega_d = \Omega$ , and  $C(x) = [\phi_1(x), \infty)$ . LVPP for this problem was previously analyzed in [85, 62]. We also consider the bilateral obstacle problem with the feasible set

$$(3.3) \quad K = \{v \in H_0^1(\Omega) \mid \phi_1 \leq v \leq \phi_2 \text{ a.e. in } \Omega\},$$

with  $C(x) = [\phi_1(x), \phi_2(x)]$ . Here,  $\phi_1, \phi_2 \in H^1(\Omega) \cap L^\infty(\Omega)$  with nonpositive and nonnegative boundary values respectively. We can choose as a Legendre function for the unilateral case the generalized Shannon entropy,

$$(3.4) \quad R(a) = (a - \phi_1) \ln(a - \phi_1) - (a - \phi_1), \text{ with } \nabla R^*(a^*) = \phi_1 + \exp a^*,$$

and for the bilateral case, the generalized Fermi–Dirac entropy,

$$(3.5) \quad \begin{aligned} R(a) &= (a - \phi_1) \ln(a - \phi_1) + (\phi_2 - a) \ln(\phi_2 - a), \\ \text{with } \nabla R^*(a^*) &= \frac{\phi_1 + \phi_2 \exp a^*}{1 + \exp a^*}. \end{aligned}$$

The resulting saddle point formulation (in weak form) is: for  $\psi^0 = 0$ , find  $(u^k, \psi^k) \in H_0^1(\Omega) \times L^\infty(\Omega)$  satisfying

$$(3.6a) \quad \alpha_k (\nabla u^k, \nabla v) + (\psi^k, v) = \alpha_k (f, v) + (\psi^{k-1}, v),$$

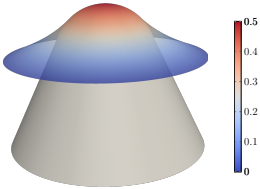
$$(3.6b) \quad (u^k, w) - (\nabla R^*(\psi^k), w) = 0,$$

for all  $(v, w) \in H_0^1(\Omega) \times L^\infty(\Omega)$ . Here and throughout,  $(\cdot, \cdot)$  denotes the  $L^2(\Omega)$  inner product. Discretizing this problem requires choosing approximation spaces for  $H_0^1(\Omega)$  and  $L^\infty(\Omega)$ , which is a standard procedure that is much more straightforward than directly discretizing the feasible sets (3.2) or (3.3). In the Galerkin finite element method, the pair of approximating spaces must satisfy a compatibility condition (cf. [85, §4.7]), but many standard choices of finite elements work, including, among others, equal-order continuous Lagrange elements for both  $u$  and  $\psi$ . As in [Section 2.3](#), we refer to these Galerkin finite element discretizations as proximal Galerkin methods.

Proximal Galerkin methods always deliver two solutions,  $u_h$  and  $\tilde{u}_h := \nabla R^*(\psi_h)$ , with the latter bound preserving by construction. Moreover, they typically exhibit mesh-independent convergence and can converge superlinearly with the number of outer iterations  $k$  if the step sizes  $\alpha_k$  are chosen appropriately (cf. (2.5)). The PDE subproblems (3.6) are straightforward to implement in standard finite element software and can be discretized with arbitrary-degree polynomial bases, if appropriate.

Method	Degree $p = 1$			Degree $p = 2$		
	$h$	$h/2$	$h/4$	$h$	$h/2$	$h/4$
Proximal Galerkin	15	13	12	15	16	12
Active Set [26, 102]	11	16	25	Not bound preserving		
Trust-Region Method [68]	6	12	19			
Interior Point (IP) [131]	9	9	8			
IP without Hessian [131]	90	260	500			

(a) Number of linear system solves for popular solvers using various mesh sizes  $h$ .



(b) Obstacle  $\phi$  (grey) and membrane  $u$  (red/blue).

Mesh size $h$	$2^{-1}$	$2^{-2}$	$2^{-3}$	$2^{-4}$	$2^{-5}$	$2^{-6}$
Finite Difference	10	15	13	15	16	16
Degree $p$	8	16	24	32	40	48
Spectral Method	16	17	16	16	16	15

(c) Number of linear system solves for the proximal finite difference and spectral methods.

Fig. 2: Example 1. The unilateral obstacle problem with the setup (3.7).

We now compare proximal Galerkin with other popular solvers. We consider the benchmark unilateral obstacle problem from [85, Experiment 4], where

$$(3.7) \quad \begin{aligned} \Omega &= \{(x, y) \in \mathbb{R}^2 : 0 < r < 1\}, \quad r^2 = x^2 + y^2, \quad f \equiv 0, \\ \phi(x, y) &= \begin{cases} \sqrt{1/4 - r^2} & r \leq b, \\ d + b^2/d - br/d & r > b, \end{cases} \quad b = 9/20, \quad d = \sqrt{1/4 - b^2}. \end{aligned}$$

We plot the obstacle and solution in Figure 2b. We use equal-order continuous Lagrange elements to discretize the solution  $u$  and the latent variable  $\psi$ . The proximal parameter  $\alpha_k$  is updated with a heuristic double-exponential rule; i.e., for all  $k \in \mathbb{N}$ , we set

$$(3.8) \quad \alpha_k = \min(\max(r^{q^k} - \alpha_{k-1}, 1), 10^2), \quad r = q = 3/2, \quad \text{and } \alpha_0 = 1.$$

Note that we do not require the proximal step size parameter  $\alpha_k$  to pass to infinity with  $k$ . In Figure 2a, we report the number of linear system solves required by the proximal Galerkin method as well as an active set strategy [26, Alg. 3.1] found in the popular scientific computing toolkit PETSc [19]<sup>1</sup>, IPOPT [131], an interior point method, with and without Hessian access, and the bound-constrained trust-region method (TRB) as implemented in GALAHAD [68]. The practical benefits of proximal Galerkin are immediately clear; the other methods, except IPOPT with Hessian access, exhibit mesh dependence. While the interior point method performs the fewest linear solves, proximal Galerkin is the only solver that also preserves bounds for higher-order discretizations. Note that by providing the Hessian matrix to IPOPT we also simultaneously provide the correct discrete Riesz map, which is known to often restore mesh independence in solvers for PDE-constrained optimization problems [121].

<sup>1</sup>The active set method [26, Alg. 3.1] can be interpreted as a semismooth Newton method for the discretized obstacle problem. However, the optimality conditions are, in general, insufficiently regular to define its infinite-dimensional formulation; see Section 1.

The LVPP saddle point subproblem (3.6) can be discretized with many other techniques. We also provide results where the subproblem (3.6) is discretized with a coefficient-based Zernike sparse spectral method [39, 109, 130, 106] and a five-point stencil finite difference method. For the finite difference scheme, we change the domain to the square  $\Omega = (-1, 1)^2$ . Here, we again use the double-exponential update rule (3.8) for  $\alpha_k$ . We terminate once  $\|\mathbf{u}_k - \mathbf{u}_{k-1}\|_{\ell^2} < 10^{-9}$  where  $\mathbf{u}_k$  is the discrete coefficient vector for  $u$  at iteration  $k$ . The results are provided in Figure 2c where we observe  $h$ - and  $p$ -independent iteration counts for the proximal finite difference and spectral methods, respectively. Further numerical experiments with the obstacle problem can be found in [85, 62, 108].

**3.2. Example 2: The Signorini problem.** We now consider the classical Signorini problem. This problem demonstrates for the first time an extension of LVPP to pointwise bound constraints acting solely on the boundary of a computational domain  $\Omega \subset \mathbb{R}^3$ . In this problem, we separate the boundary  $\partial\Omega = \bar{\Gamma}_D \cup \bar{\Gamma}_T$  into disjoint measurable subsets for imposing displacement and traction boundary conditions.

The Signorini problem, posed by Signorini in 1959 [123] and analyzed by Fichera in 1963 [59], is the essential first problem in contact mechanics. It models the deformation of a linear elastic body in the presence of a contact boundary constraint. The problem is posed on

$$(3.9) \quad V = \{u \in H^1(\Omega, \mathbb{R}^3) \mid u = g \text{ on } \Gamma_D\},$$

and involves the minimization of the strain energy function

$$(3.10) \quad J(u) = \frac{1}{2} \int_{\Omega} (\mathbf{C} \epsilon(u)) : \epsilon(u) \, dx - \int_{\Omega} f \cdot u \, dx,$$

over the feasible set

$$(3.11) \quad K = \{u \in V \mid u \cdot \tilde{n} \leq \phi_1 \text{ on } \Gamma_T\}.$$

Here,  $\epsilon : H^1(\Omega, \mathbb{R}^3) \rightarrow L^2(\Omega, \mathbb{R}_{\text{sym}}^{3 \times 3})$ ,  $\epsilon := (\nabla + \nabla^\top)/2$  denotes the symmetric gradient,  $\mathbf{C} : \mathbb{R}_{\text{sym}}^{3 \times 3} \rightarrow \mathbb{R}_{\text{sym}}^{3 \times 3}$  denotes the symmetric positive-definite elasticity tensor,  $f : \Omega \rightarrow \mathbb{R}^3$  is an internal body force density,  $\phi_1 : \Gamma_T \rightarrow \mathbb{R}_+$  is a prescribed gap function, and  $\tilde{n} : \Gamma_T \rightarrow \mathbb{R}^3$  is a prescribed vector field. For simplicity of presentation, we assume that the displacement boundary conditions are homogeneous ( $g = 0$ ) in the formulation below.

Notice that  $K$  is obtained from the general feasible set (2.1) by choosing  $V$  as in (3.9),  $B = -\gamma(\cdot) \cdot \tilde{n}$ ,  $\Omega_d = \Gamma_T$ , and  $C(x) = [\phi_1(x), \infty)$ . Applying LVPP with the Legendre function (3.4), the resulting saddle-point formulation (2.7) is: for  $\psi^0 = 0$ , find  $(u^k, \psi^k) \in V \times L^\infty(\Gamma_T)$  satisfying

$$(3.12a) \quad (\alpha_k \mathbf{C} \epsilon(u^k), \epsilon(v)) - (\psi^k, v \cdot \tilde{n})_{\Gamma_T} = (\alpha_k f, v) - (\psi^{k-1}, v \cdot \tilde{n})_{\Gamma_T},$$

$$(3.12b) \quad (u^k \cdot \tilde{n}, w)_{\Gamma_T} + (\exp \psi^k, w)_{\Gamma_T} = (\phi_1, w)_{\Gamma_T},$$

for all  $(v, w) \in V \times L^\infty(\Gamma_T)$ , where  $(\cdot, \cdot)_{\Gamma_T}$  denotes the  $L^2(\Gamma_T)$ -inner product.

As for the obstacle problem in Subsection 3.1, we use equal-order continuous Lagrange spaces for the displacement and latent variable. Note that the spaces arising in (3.12) are defined on manifolds of differing dimensions. This is inherited in the discretization, and hence, the two discrete subspaces are not the same. We use the mixed-dimensional assembly routines in DOLFINx [23, 49] to solve the coupled problem. The discrete problem is solved for a half sphere with a fixed displacement on

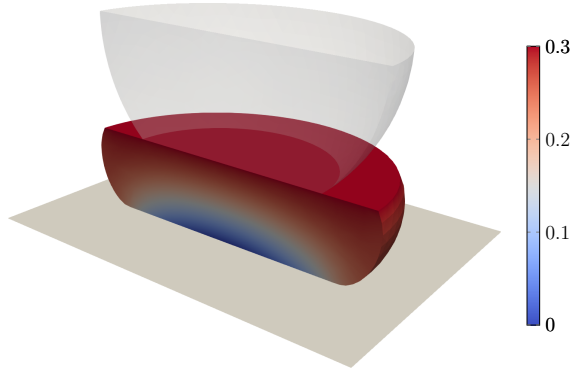


Fig. 3: Example 2. Final solution of the Signorini problem from [Subsection 3.2](#). The undeformed configuration is shown in transparency. Both have been clipped vertically to emphasize the internal displacement (colored).

the top surface, coming into contact with a rigid plane ( $\phi_1 = 0$ ). The displacement of the object and the rigid plane is visualized in [Figure 3](#). Second-order Lagrange elements approximate the geometry, the displacement, and the latent variable. The initial proximity parameter  $\alpha_0 = 0.005$  is doubled at each subsequent proximal step. The tolerance for Newton’s method is set to  $10^{-6}$ . The LVPP algorithm requires a total of 13 proximal iterations amounting to 17 linear solves. The maximum number of Newton steps was 5, the minimum 1. The number of degrees of freedom was 17,613 for a mesh with 3,661 cells.

**3.3. Example 3: Variational fracture.** The variational theory of brittle fracture of Francfort & Marigo [\[61\]](#) is formulated in terms of a function  $u$  over a domain  $\Omega$  (representing the displacement) and an unknown subset  $\Gamma \subset \Omega$  (representing the crack). The phase-field approach to fracture pioneered by Bourdin, Francfort & Marigo [\[33\]](#) approximates the crack set  $\Gamma$  with an order parameter  $c: \Omega \rightarrow [0, 1]$ , where 0 represents the undamaged state and 1 represents the complete presence of a crack, with the localization of the crack controlled by a length scale  $\ell > 0$ .

The first major challenge with solving the resulting system is that it arises from a non-convex optimization problem. In fact, several fracture problems are known to possess multiple, physically-relevant solutions [\[65\]](#). However, the objective function is biconvex, in that the problem in  $u$  or  $c$  is convex if the other variable is fixed. This inspires the most popular algorithm for its solution, alternating minimization [\[33\]](#), which iterates between minimizing only over displacement and damage, respectively. While convenient, alternating minimization can be difficult to apply to more complex physical models that lack this biconvex structure.

The second major challenge is that the numerical solution of phase-field fracture problems demands very high resolution. Experience shows that the mesh size  $h$  for the discretization must be on the order of the crack localization length scale  $\ell$ , which is typically much smaller than the diameter of  $\Omega$  for realistic simulations. These resolution requirements place a premium on mesh-independent algorithms.

We consider the anti-plane shear test formulated by Burke et al. [\[38\]](#), which exhibits multiple solutions [\[65\]](#). This problem is formulated only in terms of the vertical displacement of the body, as opposed to the full displacement typically used for other problems, but this is not central. The resulting variational inequality is closely related to the Ambrosio–Tortorelli approximation of the Mumford–Shah functional

[101, 10].

The crack evolution is computed over a quasi-static incremental loading procedure. At each step, the load on the body is varied, and the body is allowed to equilibrate. Mathematically, at each loading step, we are given Dirichlet boundary data  $g$  and the previous order parameter  $c_{\text{prev}}$ . This defines our feasible set  $K$ :

$$(3.13) \quad K = \{(u, c) \in H_g^1(\Omega) \times H^1(\Omega) \mid 0 \leq c_{\text{prev}} \leq c \leq 1 \text{ a.e. in } \Omega\},$$

where

$$(3.14) \quad H_g^1(\Omega) = \{u \in H^1(\Omega) \mid \gamma u = g \text{ on } \Gamma_D\},$$

with  $\Gamma_D \subset \partial\Omega$ . Given energy release rates  $G, G_c > 0$ , the length scale  $\ell > 0$ , and an artificial residual stiffness of a fully ruptured phase  $\epsilon > 0$ , we arrive at the (non-convex) objective functional:

$$\mathcal{J}(u, c) := \frac{G}{2} \int_{\Omega} (\epsilon + (1 - \epsilon)(1 - c)^2) |\nabla u|^2 dx + \frac{G_c}{2} \int_{\Omega} \ell |\nabla c|^2 + \ell^{-1} |c|^2 dx.$$

To obtain the feasible set  $K$  (3.13) from (2.1), we select  $V = H_g^1(\Omega) \times H^1(\Omega)^2$ ,  $B = (0, \text{id})$ , with 0 denoting the zero operator,  $\Omega_d = \Omega$ , and  $C(x) = \mathbb{R} \times [c_{\text{prev}}(x), 1]$ . Since there is no inequality constraint on the displacement variable  $u$ , we introduce only a single latent variable  $\psi$  corresponding to the damage  $c$ . We then use the Fermi–Dirac entropy (3.5) with  $\phi_1 = c_{\text{prev}}$  and  $\phi_2 = 1$ , giving us the following LVPP saddle point problem: for  $\psi^0 = 0$ , find  $(u^k, c^k, \psi^k) \in H_g^1(\Omega) \times H^1(\Omega) \times L^\infty(\Omega)$  such that

$$(3.15a) \quad \alpha_k G((\epsilon + (1 - \epsilon)(1 - c^k)^2) \nabla u^k, \nabla v) = 0,$$

$$(3.15b) \quad \alpha_k G((1 - \epsilon)(1 - c^k) |\nabla u^k|^2, d) + \alpha_k G_c(\ell(\nabla c^k, \nabla d) + \ell^{-1}(c^k, d)) + (\psi^k, d) = (\psi^{k-1}, d),$$

$$(3.15c) \quad (c^k, w) - \left( \frac{c_{\text{prev}} + \exp(\psi^k)}{\exp(\psi^k) + 1}, w \right) = 0,$$

for all  $(v, d, w) \in H_0^1(\Omega) \times H^1(\Omega) \times L^\infty(\Omega)$ .

The anti-plane shear test imposes  $u = +L$  on the top-right boundary (to the right of the initial notch) and  $u = -L$  on the top-left (to the left of the notch), Figure 4. At each loading step, the imposed displacement  $L$  is incremented by 0.005, starting from zero. Natural boundary conditions are imposed on the remainder of the boundary.

Using continuous piecewise linear finite elements for  $u$ ,  $c$ , and  $\psi$ , we solve the resulting discrete systems with Newton’s method. For robustness of the optimization procedure, a perturbed Jacobian is employed, with the addition of  $\iota((u, v) + (c, d) - (\psi, w))$  with  $\iota = 10^{-3}$ . The proximity parameter  $\alpha_k$  is updated using a simple heuristic based on the number of Newton iterations needed to solve the previous subproblem: if the number of Newton iterations is four or fewer,  $\alpha_{k+1} = 2\alpha_k$ ; if the number of Newton iterations is ten or more,  $\alpha_{k+1} = \alpha_k/2$ ; otherwise  $\alpha_{k+1} = \alpha_k$ . On average, we require 2.85 proximal steps per loading step, although with a large variance; the worst loading step took 147 proximal steps, with the second worst taking 10. Each proximal step required, on average, 5.44 Newton steps. The final damage field at  $L = 2$  is depicted in Figure 4.

<sup>2</sup>This is an affine Banach space, not a Banach space, but the arguments of Section 1 carry over, mutatis mutandis.

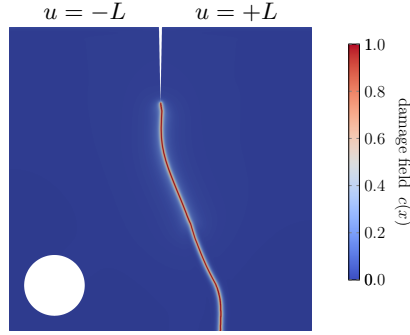


Fig. 4: Example 3. The final damage field for the fracture problem described in Subsection 3.3.

**3.4. Example 4: Vector-valued multiphase problems.** Many challenging physical problems include multiple phases, materials, or components that are required to be balanced throughout the domain. For example, reservoir simulation in petroleum engineering [57, Chap. 3], distillation columns in chemical engineering [31, Chap. 11], and optimal design in semiconductors [1], all explicitly require such constraints. From a mathematical perspective, the state variables, whether they be materials, components, or concentrations in the domain  $\Omega$  are represented by vector-valued functions  $u: \Omega \rightarrow \mathbb{R}^m$ , where  $m$  denotes the number of states. The natural feasible set for such systems is a Gibbs simplex over a specified function space  $V$ ; namely,

$$(3.16) \quad K(V) := \left\{ u \in V \mid \sum_{i=1}^m u_i(x) = 1 \text{ and } u_i(x) \geq 0 \text{ (} i = 1, \dots, m \text{) f.a.e. } x \in \Omega \right\}.$$

This feasible set  $K = K(V)$  fits into our framework by setting  $B = \text{id}$ ,  $\Omega_d = \Omega$ , and  $C = \{a \in \mathbb{R}^m \mid \sum_{i=1}^m a_i = 1, a_i \geq 0\}$ . In this case, the LVPP subproblem has a relation  $u = \nabla R^*(\psi)$  induced by the Legendre function

$$(3.17) \quad R(a) = \sum_{i=1}^m a_i \ln(a_i), \quad \text{with} \quad \frac{\partial R^*}{\partial a_i^*}(a^*) = \frac{\exp(a_i^*)}{\sum_{j=1}^m \exp(a_j^*)} \text{ for each } i = 1, \dots, m,$$

which couples the components of the primal variable  $u: \Omega \rightarrow C \subset \mathbb{R}^m$  (the states) to the vector-valued latent variable  $\psi: \Omega \rightarrow [-\infty, \infty]^m$ .

For our numerical example, inspired by [63], we construct a Cahn–Hilliard-type gradient flow toward a constrained minimizer of the Ginzburg–Landau-type energy functional

$$I(u) = \int_{\Omega} \frac{\varepsilon^2}{2} \sum_{i=1}^m |\nabla u_i|^2 + W(u) \, dx, \quad W(u) = \sum_{i=1}^m u_i(1 - u_i) + i_K(u),$$

where  $i_K(u) = 0$  if  $u \in K$  and  $i_K(u) = +\infty$  otherwise denotes the indicator function for  $K$ . Here,  $\varepsilon > 0$  is a diffuse interface parameter that controls the width of the region containing mixed states. The seminal works of Modica [98, 99] demonstrate that functionals of this type tend (in the sense of  $\Gamma$ -convergence [47]) to a functional measuring the perimeter of the phase boundaries as  $\varepsilon \rightarrow 0$ . Therefore, the Ginzburg–Landau energy acts as a penalty on pathological free boundaries (phase transitions) and favors straight edges. This model problem can be easily modified with more

complex energy functionals that, for instance, reflect anisotropic behavior amongst the various components represented by  $u$  [64].

The chosen gradient flow over  $\Omega$  is described by the system of differential inclusions

$$\frac{du}{dt} \in -\varepsilon^2 \Delta^2 u + \Delta \partial W(u),$$

where  $\partial$  denotes the Clarke subdifferential of the nonsmooth functional  $W$  [44, Chap. 2]. Using backward Euler to discretize this system in time is equivalent to solving a recursive sequence of minimization problems over the feasible set (3.16) with  $V = H^2(\Omega)$ . In particular, at each time step, we minimize

$$(3.18) \quad J(u) = \frac{1}{2} \int_{\Omega} |u - u_{\text{prev}}|^2 dx + \tau \int_{\Omega} \frac{\varepsilon^2}{2} \sum_{i=1}^m (\Delta u_i)^2 + \Delta W(u) dx,$$

where  $\tau > 0$  is the width of the time step, and  $u_{\text{prev}}$  is the solution at the previous point in time. We can readily apply LVPP to these semi-discrete subproblems.

As is often done in practice, see, e.g., [54], we avoid discretizing the natural function space for  $u$ , namely  $H^2(\Omega; \mathbb{R}^m)$ , by introducing slack variables  $z_i = \varepsilon^2 \Delta u_i - [\partial W(u)]_i$ . Given the previous solution  $u_{\text{prev}} \in H^1(\Omega; \mathbb{R}^m)$ , the LVPP subproblems take the form: for  $\psi^0 = 0$ , find  $(u^k, z^k, \psi^k) \in H^1(\Omega; \mathbb{R}^m) \times H^1(\Omega; \mathbb{R}^m) \times L^\infty(\Omega; \mathbb{R}^m)$  such that for,  $i = 1, \dots, m$ , we have

$$(3.19a) \quad \alpha_k(z_i^k, y_i) + \varepsilon^2 \alpha(\nabla u_i^k, \nabla y_i) - 2\alpha_k(u_i^k, y_i) + (\psi_i^k, y_i) = (\psi_i^{k-1}, y_i) - \alpha_k(1, y_i),$$

$$(3.19b) \quad (u_i^k, v_i) - \tau(\nabla z_i^k, \nabla v_i) = (u_{\text{prev},i}, v_i),$$

$$(3.19c) \quad (u_i^k, w_i) - \left( \frac{\exp(\psi_i^k)}{\sum_{j=1}^m \exp(\psi_j^k)}, w_i \right) = 0,$$

for all  $(v, y, w) \in H^1(\Omega; \mathbb{R}^m) \times H^1(\Omega; \mathbb{R}^m) \times L^\infty(\Omega; \mathbb{R}^m)$ . Note that LVPP generates two semi-discrete flows using the primal variables  $u(t_1), u(t_2), \dots$  and the latent solutions  $\tilde{u}(t_1), \tilde{u}(t_2), \dots$  for the time steps  $0 \leq t_1 < t_2 < \dots$ , where each  $\tilde{u}_i := \frac{\exp(\psi_i^k)}{\sum_{j=1}^m \exp(\psi_j^k)}$  arises from (3.19c). The latent flow satisfies the constraints in  $K$  even after discretizing (3.19) in space.

In our numerical experiments, we solve (3.19) on a square domain in  $\mathbb{R}^2$  with Neumann/natural boundary conditions imposed on  $u$  and  $z$ . We increment the differential inclusion with a time step of size  $\tau = 10^{-5}$  and start from an initial array of  $m = 4$  phases that sum to one throughout the domain, inspired by [139, Sec. 4.3].

We discretize the underlying function spaces by piecewise linear continuous finite elements and solve the resulting discrete subproblems with Newton's method to a tolerance of  $10^{-8}$ . The proximity parameter  $\alpha_k = 1$  is kept constant. On average, we require 8 proximal steps per time step, where the maximum number of proximal steps over all time intervals was 8 and the minimum 7. The average number of linear solves per Newton iteration was 2, resulting in roughly 16 linear solves per time step. We plot several snapshots of the evolution in Figure 5.

**3.5. Example 5: Obstacle-type quasi-variational inequalities.** Obstacle-type quasi-variational inequalities (QVIs) [8] introduce an additional layer of complexity to the modeling framework. Here, the pointwise state constraints are no longer fixed but rather depend on the solution itself, which substantially contributes to the nonsmooth and nonlinear characteristics of the problem. The extremely versatile nature of QVIs makes them the model of choice for a number of important problems in

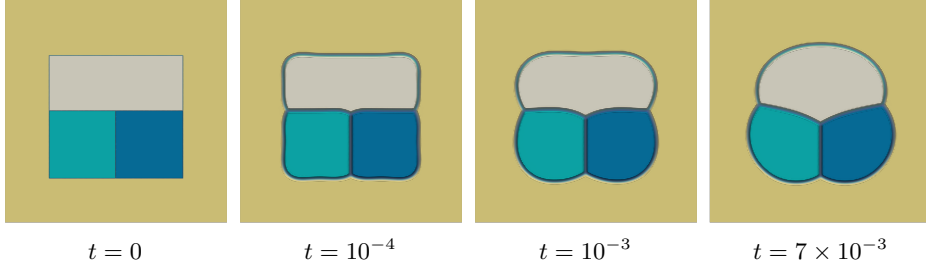


Fig. 5: Example 4. The evolution of the four phases  $u_i$ ,  $i = 1, 2, 3$ , of the Cahn–Hilliard problem described in Subsection 3.4 at times  $t = 0, 10^{-4}, 10^{-3}$ , and  $7 \times 10^{-3}$ .

physics and economics [7, 16, 18, 27, 28, 95, 100]. However, this structure also means their numerical treatment poses a significant challenge, and the literature on solvers that tackle infinite-dimensional QVIs is limited. Fixed point methods are popular [3, 8] but require that the QVI be reformulated as a fixed point problem with a contraction. This restricts its application to a small subclass of QVIs, and even if there is a contraction, the contraction coefficient may be close to one, requiring a computationally infeasible number of iterations for convergence. Alternative methodologies include the use of penalty methods [8, 36], augmented Lagrangian methods [82], or active set strategies [6], which may be mesh-independent but either produce infeasible solutions or are confined to nodal low-order discretizations.

We now investigate the application of LVPP to QVIs. Since the obstacle appears explicitly in the equations to be solved in LVPP, it may, therefore, be treated in a straightforward manner as a function of the unknown solution. We restrict our discussion to a class of obstacle-type QVIs known as thermoforming problems [7, 8, 134]. The objective of the thermoforming QVI is to find the equilibrium between a plastic membrane  $u \in H_0^1(\Omega)$  pushed upwards by a force  $f \in L^2(\Omega)$  and heated to a temperature  $T \in H^1(\Omega)$  into a metallic mold denoted by  $\Phi \in H^1(\Omega)$ . In this case,  $\Phi := \Phi_0 + \xi T$ , where  $\Phi_0 \in H^1(\Omega)$  is the initial shape of the mold and  $\xi \in C^2(\bar{\Omega}) \cap H_0^1(\Omega)$  is a given smoothing function. Unlike in the obstacle problem of Subsection 3.1, where the obstacle is fixed, the mold deforms due to the heat of the membrane, causing it to expand upwards. The deformation of the mold is modeled by a nonlinear screened Poisson equation that ensures a larger heat transfer from the membrane to the mold in regions where they are in close contact. The behavior of the heat transfer is dictated by a positive conduction coefficient  $\beta > 0$  and a given globally Lipschitz non-increasing function  $g: \mathbb{R} \rightarrow \mathbb{R}$  that defines an operator  $g: H^1(\Omega) \rightarrow H^1(\Omega)$  (not relabeled). We define the feasible set as

$$(3.20) \quad K(T) := \{v \in H_0^1(\Omega) \mid v \leq \Phi = \Phi_0 + \xi T\}.$$

The thermoforming QVI problem is to find  $(u, T) \in H_0^1(\Omega) \times H^1(\Omega)$  that satisfies for all  $(v, q) \in K(T) \times H^1(\Omega)$ ,

$$(3.21a) \quad (\nabla T, \nabla q) + \beta(T, q) = (g(\Phi_0 + \xi T - u), q),$$

$$(3.21b) \quad (\nabla u, \nabla(v - u)) \geq (f, v - u).$$

As in Subsection 3.1, we choose the generalized Shannon entropy (3.4) for the Legendre function in the LVPP subproblems (but with the relevant signs switched as we are dealing with a unilateral upper bound rather than a lower bound). The resulting saddle point formulation (in weak form) is: for  $\psi^0 = 0$ , find  $(u^k, \psi^k, T^k) \in$

$H_0^1(\Omega) \times L^\infty(\Omega) \times H^1(\Omega)$  satisfying for all  $(v, w, q) \in H_0^1(\Omega) \times L^\infty(\Omega) \times H^1(\Omega)$ ,

$$(3.22a) \quad (\nabla T^k, \nabla q) + \beta(T^k, q) = (g(\exp(-\psi^k)), q),$$

$$(3.22b) \quad \alpha_k(\nabla u^k, \nabla v) + (\psi^k, v) = \alpha_k(f, v) + (\psi^{k-1}, v),$$

$$(3.22c) \quad (u^k, w) + (\exp(-\psi^k), w) = (\Phi_0 + \xi T^k, w).$$

The first equation (3.22a) arises thanks to the pointwise equality in (3.22c) and may also be rewritten as

$$(3.22a') \quad (\nabla T^k, \nabla q) + \beta(T^k, q) = (g(\Phi_0 + \xi T^k - u^k), q),$$

which corresponds to (3.21a) in the original QVI problem. We choose the former formulation as it achieves slightly better numerical convergence.

We now fix the parameters:  $\Omega = (0, 1)^2$ ,  $\beta = 1$ ,  $\xi(x, y) = \sin(\pi x) \sin(\pi y)$ ,  $f \equiv 25$ ,  $\Phi_0(x, y) = 1 - 2 \max(|x - 1/2|, |y - 1/2|)$ , and

$$g(s) = \begin{cases} 1 & s \leq 0, \\ 1 - 100s & 0 < s < 10^{-2}, \\ 0 & s \geq 10^{-2}. \end{cases}$$

A continuous piecewise linear finite element discretization is chosen for  $u$ ,  $\psi$ , and  $T$  with mesh size  $h = 0.01$ . We initialize the algorithm with  $(u^0, T^0) \equiv (0, 1)$ ,  $\alpha_1 = 2^{-6}$  and adopt the update rule  $\alpha_{k+1} = 4\alpha_k$ . The algorithm terminates once  $\|u^k - u^{k-1}\|_{H^1(\Omega)} \leq 10^{-9}$ . For robustness, a small Jacobian modification is added corresponding to  $-10^{-10} \alpha_k^{-1} (\nabla \psi^k, \nabla w)$ . Convergence was reached after solving 17 LVPP subproblems, reaching  $\alpha_{17} = 2^{26}$ , requiring a total of 25 Newton iterations averaging at 1.47 iterations per LVPP subproblem. The maximum number of Newton iterations for an LVPP subproblem was four and the smallest was one. We plot the solutions in Figure 6. Using the same termination criterion, a fixed point method requires 329 fixed point iterations to reach convergence, where each outer fixed point iteration requires both a nonlinear PDE solve to compute  $T^{k+1}$  (given a  $u^k$ ) followed by an obstacle problem solve to compute  $u^{k+1}$ . Thus, in the best-case scenario, one requires at least 658 Newton iterations to reach convergence (although the linear systems are smaller than the LVPP subproblems). In reality, the number of Newton iterations involved is significantly larger since each fixed point iteration requires more than two Newton iterations. From these preliminary results, it appears that LVPP is a promising choice for the numerical solution of QVIs.

**4. Beyond bound constraints.** We continue our study of LVPP by considering pointwise gradient and eigenvalue constraints. These are important but less well-studied classes of problems, with fewer competing methods available. The Lagrange multipliers for gradient constraints are much less regular than with bound constraints and, hence, much more subtle to discretize. In particular, the higher regularity of the solution  $u$  does not necessarily carry over to more regular Lagrange multipliers, as is often exploited to develop methods for pointwise bound constraints. In addition, whereas one can, e.g., enforce a function's non-negativity using non-negative bases and coefficients, it is very difficult to enforce gradient or eigenvalue constraints by designing suitable bases.

We consider three representative problems. The first is a simple plasticity model involving constraints on the norm of the gradient of a function  $u: \Omega \rightarrow \mathbb{R}$ . The second

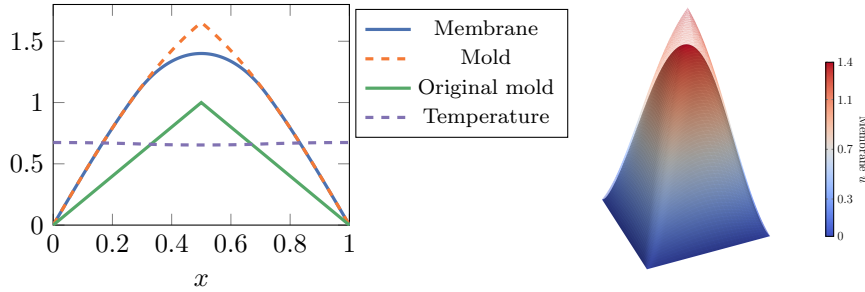


Fig. 6: Example 5. (Left) One-dimensional slice of the membrane  $u$  at  $y = 1/2$ , mold  $\Phi$ , original mold  $\Phi_0$ , and temperature  $T$  for the QVI problem described in [Subsection 3.5](#). (Right) Surface plot of the membrane  $u$  (solid) and mold  $\Phi$  (wireframe).

considers enforcing natural bounds on the eigenvalues of an orientation variable in the Landau–de Gennes model for nematic liquid crystals. The third demonstrates the treatment of intersections of inequality constraints using an obstacle problem with an additional gradient norm constraint.

**4.1. Example 6: Gradient norm constraints.** Constraints on the gradient of the state are well-known from the optimal control literature; see, e.g., [136, 96, 41, 76, 137], where they are often used as a simplified model of a stress constraint. They also appear in the literature on (quasi-)variational inequalities; see the recent survey [118] and the references therein. In particular, this type of constraint has been used to model the elastic-plastic torsion problem [127, 35], sandpile growth [112, 13], magnetization in type-II superconductors [111], and in hydrology [110]. Though the literature is decidedly more scarce for numerical methods for these types of variational inequalities compared to say the obstacle problem, a quadratic penalty semismooth Newton approach has been successfully employed before, see e.g., [77].

Given a domain  $\Omega \subset \mathbb{R}^n$  and a function  $\phi \in L^\infty(\Omega)$  such that  $\phi \geq \epsilon$  a.e. for some constant  $\epsilon > 0$ , a typical feasible set for gradient constraints is

$$(4.1) \quad K = \{u \in H_0^1(\Omega) \mid |\nabla u| \leq \phi \text{ a.e. in } \Omega\}.$$

To obtain this feasible set  $K$  from (2.1), we set  $V = H_0^1(\Omega)$ ,  $B = \nabla$ ,  $C(x)$  equal to the Euclidean ball of radius  $\phi(x)$ , and  $\Omega_d = \Omega$ . For some  $f \in L^2(\Omega)$ , we consider minimizing the Dirichlet energy  $J$ , as defined in (3.1), in  $K$ . We use a modification of the Hellinger entropy [126], which captures the geometry of the Euclidean ball, as the Legendre function:

$$(4.2) \quad R(a) := -\sqrt{\phi^2 - |a|^2}, \text{ with } \nabla R^*(a^*) = \frac{\phi}{\sqrt{1 + |a^*|^2}} a^*.$$

This leads to the following LVPP saddle point problem: for  $\psi^0 = 0$ , find  $(u^k, \psi^k) \in H_0^1(\Omega) \times L^\infty(\Omega, \mathbb{R}^n)$  such that

$$(4.3a) \quad \alpha_k(\nabla u^k, \nabla v) + (\psi^k, \nabla v) = \alpha_k(f, v) + (\psi^{k-1}, \nabla v),$$

$$(4.3b) \quad (\nabla u^k, w) - \left( \frac{\phi \psi^k}{\sqrt{1 + |\psi^k|^2}}, w \right) = 0$$

for all  $(v, w) \in H_0^1(\Omega) \times L^\infty(\Omega, \mathbb{R}^n)$ .

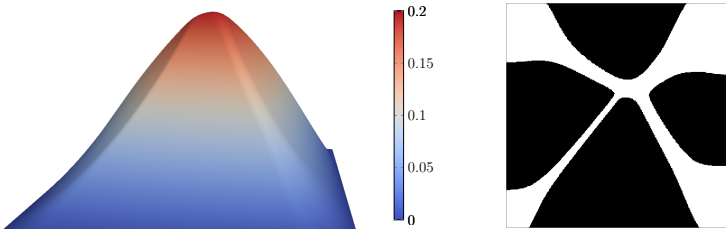


Fig. 7: Example 6. Left: the discretized solution variable  $u_h(x)$ . Right: the estimated active set based on  $\nabla R^*(\psi_h)$  (black). The algorithm was stopped once  $\|u_h^k - u_h^{k-1}\|_{L^2(\Omega)} < 10^{-8}$ .

For our numerical experiments, we solve (4.3) on a unit square domain in  $\mathbb{R}^2$  with homogeneous Dirichlet boundary conditions imposed on  $u$ . We set

$$f(x_1, x_2) := 15 \sin^2(\pi x_1) \quad \text{and} \quad \phi(x_1, x_2) := 0.1 + 0.2x_1 + 0.4x_2$$

for all  $(x_1, x_2) \in \Omega$ . We then discretize the underlying function spaces using continuous piecewise quadratic finite elements for  $u$  and continuous piecewise linear finite elements for the latent variable  $\psi$ . The stopping condition on (4.3) is the  $L^2(\Omega)$ -norm of the increment in the primal variable from one proximal step to the next,  $\|u_h^k - u_h^{k-1}\|_{L^2(\Omega)} < \text{tol.}$ , with the tolerance set to  $10^{-8}$ . The proximity parameter begins with  $\alpha_1 = 1$  and doubles at each new proximal step. The tolerance for Newton's method is set to  $10^{-8}$ . For a mesh of  $200 \times 200$  cells, the method requires a total of 17 proximal iterations amounting to 27 linear solves. The maximum number of Newton steps was 4, and the minimum was 1, with the final 12 iterations requiring only one Newton step per proximal iteration. We plot the computed solution and approximated active set Figure 7. For the latter, we plot the characteristic function for the set where  $|\nabla R^*(\psi_h)| \geq \phi - 10^{-8}$ .

**4.2. Example 7: Eigenvalue constraints.** We illustrate how to apply LVPP to enforce eigenvalue bounds. This class of constraints is very difficult to enforce but also very important in engineering design.

As a didactic example, we enforce the eigenvalue constraints of the Landau–de Gennes model for nematic liquid crystals. In this model, the orientation of the liquid crystal is described by a tensor-valued order parameter  $Q(x)$  [48, 20, 132]. More specifically, on a domain  $\Omega \subset \mathbb{R}^n$ , at each point  $Q$  is a symmetric and traceless  $n \times n$  matrix, and must satisfy the eigenvalue constraints

$$(4.4) \quad \lambda_i(Q) \in [-1/n, (n-1)/n], \quad i = 1, \dots, n.$$

The equilibrium configuration of the liquid crystal is attained by solving a minimization problem with a suitable energy functional. In almost all cases, the eigenvalue constraints are not explicitly enforced in the numerical optimization (e.g., [114, 125]), although they are usually satisfied through careful choice of the bulk energy term [21, 97, 20]. A notable exception is the barrier approach of Wang & Xu [133], which adds a quasi-entropy to the functional to be minimized that blows up as  $\lambda(Q)$  approaches the bounds.

We consider the setup of Robinson et al. [114], with a slightly modified nondimensionalization. The problem is to minimize the energy functional

$$(4.5) \quad J(u) = \frac{1}{2} \int_{\Omega} \nabla Q : \nabla Q \, dx + \frac{1}{2} \int_{\Omega} A \operatorname{tr}(Q^2) \, dx + \frac{1}{4} \int_{\Omega} C(\operatorname{tr}(Q^2))^2 \, dx,$$

on the domain  $\Omega = (0, 1)^2$ , with parameters  $A = 1, C = 4$ . The feasible set is

$$(4.6) \quad K = \{Q \in H_g^1(\Omega, \mathbb{R}_{\text{sym, tr}}^{2 \times 2}) \mid -\frac{1}{2}I \preceq Q \preceq \frac{1}{2}I \text{ a.e. in } \Omega\}.$$

Here  $H_g^1(\Omega, \mathbb{R}_{\text{sym, tr}}^{2 \times 2})$  is the set of  $H^1$  symmetric traceless matrices enforcing the boundary condition

$$(4.7) \quad g(x, y) = \begin{pmatrix} \frac{1}{2}s(x, y) \cos(2\theta) & \frac{1}{2}s(x, y) \sin(2\theta) \\ \frac{1}{2}s(x, y) \sin(2\theta) & -\frac{1}{2}s(x, y) \cos(2\theta) \end{pmatrix},$$

where  $\theta = 0$  on  $y \in \{0, 1\}$ ,  $\theta = \pi/2$  on  $x \in \{0, 1\}$ , and the nematic ordering  $s$  ramps to zero at the corners:

$$(4.8) \quad s(x, y) = \begin{cases} T(x) & y \in \{0, 1\}, \\ T(y) & x \in \{0, 1\}, \end{cases}$$

with ramp function

$$(4.9) \quad T(z) = \begin{cases} z/d & z \in [0, d), \\ 1 & z \in [d, 1-d), \\ (1-z)/d & z \in [1-d, 1], \end{cases}$$

for ramp scale  $d = 0.06$ .

To obtain  $K$  from (2.1), we set  $V = H_g^1(\Omega, \mathbb{R}_{\text{sym, tr}}^{2 \times 2})$ ,  $B = I$ ,  $C(x)$  to be the set of all symmetric  $n \times n$  matrices with spectral radius less than or equal to  $\lambda_{\max} = 1/2$ , and  $\Omega_d = \Omega$ . We suggest selecting the entropy

$$R(a) = \text{tr} \left( (a + \lambda_{\max} I) \ln(a + \lambda_{\max} I) + (\lambda_{\max} I - a) \ln(\lambda_{\max} I - a) \right),$$

with  $\nabla R^*(a^*) = \lambda_{\max} \text{tanhm}(a^*/2)$ ,

where  $\text{tanhm}$  is the matrix tanh function. Since  $\tanh : \mathbb{R} \rightarrow (-1, 1)$ , any output of the induced matrix function  $\text{tanhm}$  has spectral radius at most one. We implement  $\text{tanhm}$  using the formula

$$(4.10) \quad \text{tanhm}(a) = 2(\exp(2a) + I)^{-1}(\exp(2a) - I)$$

and in turn implement the matrix exponential  $\exp$  using the formulae of Bernstein & So [30] for  $n = 2^3$  and Cheng & Yau [43] for  $n = 3^4$ . In particular, with a careful implementation in the symbolic Unified Form Language [5] employed by FEniCS and Firedrake, the derivatives of  $\text{tanhm}$  and  $\exp$  needed in a Newton iteration are computed automatically.

In two dimensions, since  $\tanh$  is odd, if  $a$  is traceless, then  $\text{tanhm}(a)$  is also traceless. The natural space for the latent variable is therefore  $L^\infty(\Omega, \mathbb{R}_{\text{sym, tr}}^{2 \times 2})$ <sup>5</sup>. This

<sup>3</sup>There is a minor typographical error in [30]. The prefactor in case *i*) of Corollary 2.4 should be  $\exp((a+d)/2)$ , not  $\exp(a+d/2)$ .

<sup>4</sup>There are several minor typographical errors in [43]. First, the indices  $i$  and  $j$  in (22) should be swapped. Second, the key formula (28') for the case with three distinct eigenvalues is missing several minus signs—the coefficients of  $A^2$  and  $I$  should be negated.

<sup>5</sup>For  $n > 2$  the latent variable would not necessarily be traceless.

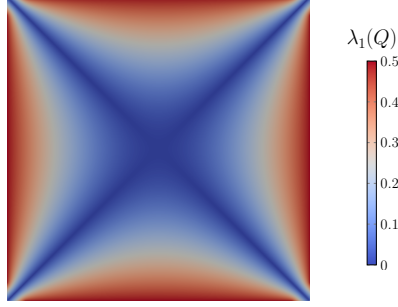


Fig. 8: Example 7. The largest eigenvalue  $\lambda_1(Q)$  of the minimizer of the Landau–Gennes energy (4.5) over (4.6). The other eigenvalue of the matrix is its negation.

leads to the following LVPP iteration: for  $\psi^0 = 0$ , find  $(Q^k, \psi^k) \in H_g^1(\Omega, \mathbb{R}_{\text{sym, tr}}^{2 \times 2}) \times L^\infty(\Omega, \mathbb{R}_{\text{sym, tr}}^{2 \times 2})$  such that

$$(4.11a) \quad \alpha_k J'(Q; V) + (\psi^k, V) = (\psi^{k-1}, V)$$

$$(4.11b) \quad (Q, w) - (\lambda_{\max} \tanh m(\psi/2), w) = 0$$

for all  $(V, w) \in H_0^1(\Omega, \mathbb{R}_{\text{sym, tr}}^{2 \times 2}) \times L^\infty(\Omega, \mathbb{R}_{\text{sym, tr}}^{2 \times 2})$ . For  $n > 2$ , (4.11b) would change to

$$(4.12) \quad (Q, w) - \left( \frac{1}{2} \tanh m(\psi/2) + \frac{n-2}{2n} I, w \right) = 0$$

to scale and shift the eigenvalues into the physical range.

We discretize with piecewise cubic continuous finite elements on a  $100 \times 100$  regular quadrilateral mesh for the components of both  $Q$  and  $\psi$ . Since both variables are symmetric and traceless, they are described by two scalar fields, i.e., we employ the ansätze

$$(4.13) \quad Q = \begin{pmatrix} Q_1 & Q_2 \\ Q_2 & -Q_1 \end{pmatrix}, \quad \psi = \begin{pmatrix} \psi_1 & \psi_2 \\ \psi_2 & -\psi_1 \end{pmatrix}.$$

The solver took 6 proximal steps, requiring a total of 11 Newton steps. The converged solution, depicted in Figure 8, satisfies the eigenvalue constraints (4.4) pointwise. The solution is the well-known well order-reconstruction solution discovered by Kralj & Majumdar [91].

**4.3. Example 8: Intersections of constraints.** It is straightforward to apply LVPP when  $K$  is defined as the intersection of several sets. We demonstrate this by minimizing the Dirichet energy  $J$ , as defined in (3.1) with  $f \equiv 0$  over the convex feasible set

$$(4.14) \quad K = \{u \in H_0^1(\Omega) \mid u \geq \phi_0 \text{ and } |\nabla u| \leq \phi \text{ a.e. in } \Omega\},$$

which can be seen as the intersection of (3.2) and (4.1). We assume  $\phi$  and  $\phi_0$  satisfy suitable consistency conditions so that solutions to this problem exist. To obtain  $K$  from (2.1), we set  $V = H_0^1(\Omega)$ ,  $B = (\text{id}, \nabla)^\top$ ,  $C(x)$  to be the Cartesian product the closed interval  $[\phi_0(x), \infty)$  and the Euclidean ball of radius  $\phi(x)$ , and  $\Omega_d = \Omega$ . The geometry of this Cartesian product is captured by adding the entropies associated

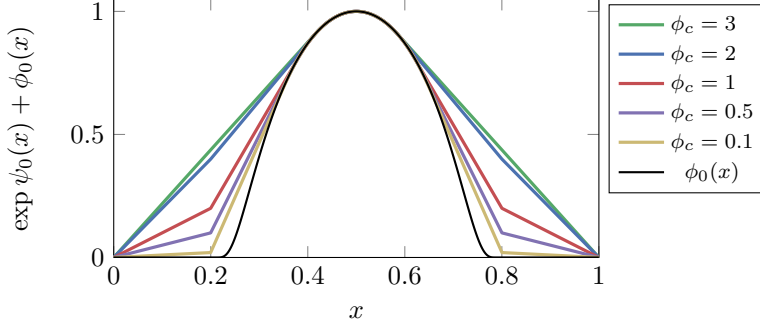


Fig. 9: Example 8. Solutions to (4.16) with both obstacle and gradient constraints. The value of  $\phi_c$  determines the gradient constraint imposed on  $[0, 0.2] \cup [0.8, 1]$ , while  $\phi_0(x)$  defines the obstacle constraint.

with the independent components:

$$(4.15) \quad R((a_0, a)) = (a_0 - \phi_0) \ln(a_0 - \phi_0) - (a_0 - \phi_0) - \sqrt{\phi^2 - |a|^2},$$

$$\text{with } \nabla R^*((a_0^*, a^*)) = \begin{pmatrix} \phi_0 + \exp a_0^* \\ \frac{\phi a^*}{\sqrt{1 + |a^*|^2}} \end{pmatrix}.$$

For fixed  $a_0$ , the geometry of the ball of radius  $\phi(x)$  is captured by the Hellinger entropy; for fixed  $a$ , the geometry of  $[\phi_0(x), \infty)$  by the Fermi–Dirac entropy.

Since the gradient isomorphism  $\nabla R^*$  has two components, we introduce two latent variables, just as a problem with two inequality constraints requires two Lagrange multipliers. This leads to the following saddle point problem: for  $(\psi_0^0, \psi^0) = (0, 0)$ , find  $(u^k, \psi_0^k, \psi^k) \in H^1(\Omega) \times L^\infty(\Omega) \times L^\infty(\Omega, \mathbb{R}^n)$  such that

$$(4.16a) \quad \alpha_k(\nabla u^k, \nabla v) + (\psi_0^k, v) + (\psi^k, \nabla v) = (\psi_0^{k-1}, v) + (\psi^{k-1}, \nabla v)$$

$$(4.16b) \quad (u^k, w_0) - (\exp \psi_0^k, w_0) = (\phi_0, w_0)$$

$$(4.16c) \quad (\nabla u^k, w) - \left( \frac{\phi \psi^k}{\sqrt{1 + |\psi^k|^2}}, w \right) = 0$$

for all  $(v, w_0, w) \in H^1(\Omega) \times L^\infty(\Omega) \times L^\infty(\Omega, \mathbb{R}^n)$ .

We solve this problem for  $\Omega = (0, 1)$ , and obstacle and gradient constraints given by

$$(4.17) \quad \phi_0(x) = \begin{cases} c \exp\left(-\frac{1}{10(x-0.2)(0.8-x)}\right) & x \in (0.2, 0.8), \\ 0 & \text{otherwise,} \end{cases}$$

$$\phi(x) = \begin{cases} \phi_c & x \in [0, 0.2] \cup [0.8, 1], \\ 100 & \text{otherwise,} \end{cases}$$

where the normalisation constant  $c \in \mathbb{R}$  is chosen so that  $\phi_0(0.5) = 1$ , and  $\phi_c > 0$  is to be varied. We discretize (4.16) with continuous piecewise linear finite elements for all variables  $(u, \psi_0, \psi)$ .

The solutions for different values of  $\phi_c$  are shown in Figure 9. We plot the obstacle-conforming approximation  $\phi_0 + \exp \psi_0$  (the primal solutions are similar). As

$\phi_c$  is reduced, the gradient constraint becomes more and more restrictive, changing both the slope on  $[0, 0.2] \cup [0.8, 1]$  and the active set in contact with the obstacle.

**5. Equality constraints.** Some of the most common constraints in computational mechanics are *equality* constraints. In this section, we demonstrate two ways LVPP can be extended to treat them. First, under appropriate assumptions, replacing  $R$  with  $\epsilon R$  and taking the limit  $\epsilon \downarrow 0$  in (2.7) delivers a variational formulation for the (nonlinear) equality constraint  $Bu(x) \in \partial C$ . As an illustrative example, we consider harmonic maps  $u: \Omega \rightarrow \mathbb{R}^m$  that satisfy the norm constraint  $|u| = 1$  [24, Chap. 7]. On the other hand, by replacing  $R^*$  with  $\epsilon R^*$  and taking the limit  $\epsilon \downarrow 0$ , we uncover the common Lagrange multiplier formulation for the (linear) equality constraint  $Bu = 0$ . This class of problems is well-studied [32], including the Stokes and Maxwell equations along with many others, so we choose not to provide a numerical example.

**5.1. Example 9: Constraining to the boundary of a convex set.** Suppose we wish to enforce  $u(x) \in \partial C$  when optimizing  $J(u)$ , where  $\partial C$  is the boundary of a closed convex set  $C \subset \mathbb{R}^m$  with non-empty interior. We begin by relaxing this *nonconvex* constraint by requiring instead that  $u(x) \in C$ . As before, given a Legendre function  $R$  and its convex conjugate  $R^*$  for the set  $C$ , the nonlinear algebraic relation for enforcing inequality constraints in the LVPP saddle point problem (2.7) is given by  $Bu = \nabla R^*(\psi)$  for some latent variable  $\psi$ .

Since  $\nabla R^*$  maps into the interior of  $C$ , it naturally excludes the boundary  $\partial C$ . However, we can rescale  $R^*$  in such a way that the limiting object resides on  $\partial C$ , at least whenever  $C$  is bounded. We do so by *epi-multiplying*  $R^*$  by a scalar  $\epsilon > 0$  [116, Chap. 5]. More specifically, we replace  $R^*(a^*)$  by  $\epsilon R^*(\epsilon^{-1}a^*)$  so that, by the chain rule, the algebraic relation in the LVPP saddle point problem (2.7b) becomes  $Bu = \nabla R^*(\epsilon^{-1}\psi)$ . On the primal level, all we have done is scale the image of  $R$  by  $\epsilon$ , but this has a profound effect on the conjugate function  $R^*$ . Passing to the limit  $\epsilon = 0$  using the pointwise limit inferior turns  $a^* \mapsto \epsilon R^*(\epsilon^{-1}a^*)$  into the recession function of  $R^*$ , a tool for predicting the behavior of a function when its argument approaches infinity [117, Chap. 3].

To see effects relevant to our derivation, fix some  $\epsilon > 0$  and  $a^* \in \mathbb{R}^n$  and let  $a_\epsilon := \nabla R^*(\epsilon^{-1}a^*) \in C$ . Since  $\nabla R^{-1} = \nabla R^*$ , we have  $\epsilon^{-1}a^* = \nabla R(a_\epsilon)$  and, consequently,  $|\nabla R(a_\epsilon)| \rightarrow +\infty$  as  $\epsilon \downarrow 0$ . For bounded sets  $C$ , this forces  $a_\epsilon$  to tend to an element in  $\partial C$  as  $\epsilon \downarrow 0$ . Indeed, if this were not the case, then given a null sequence  $\epsilon_k \downarrow 0$ , there would exist a subsequence  $a_{\epsilon_k}$  (still indexed by  $k$ ) that converges to an element  $\bar{a}$  in the interior of  $C$ . But since  $\nabla R$  is continuous on the interior of  $C$  by the definition of Legendre function, the limit  $\nabla R(\bar{a})$  would be finite, which is a contradiction.

For example, let  $\phi: \Omega \rightarrow \mathbb{R}$  be some uniformly positive function. Our abstract observations imply that the pointwise norm constraint  $|Bu| = \phi$  can be treated by replacing  $\nabla R^*(a^*)$  derived from the Hellinger entropy in (4.2) with

$$\nabla R^*(\epsilon^{-1}a^*) = \phi \frac{a^*}{\sqrt{\epsilon^2 + |a^*|^2}}$$

and taking the pointwise limit  $\epsilon \rightarrow 0$ . Indeed, observe that  $\nabla R^*(\epsilon^{-1}a^*) \rightarrow \phi a^*/|a^*|$ , requiring us to replace (2.7b) by the equation

$$(5.1) \quad Bu^k = \phi \psi^k / |\psi^k|.$$

Clearly, this ensures the constraint  $|Bu^k| = \phi$  at each subproblem  $k$ .

Differential geometry inspires the model problem in this subsection. However, the norm constraint  $|u| = 1$  also appears in modeling ferrofluids, see [92], which goes back to classical work of Landau and Lifshitz [93], and liquid crystals [124]. In each case, we must set  $B = \text{id}$  and  $\phi = 1$  in (5.1). Roughly speaking, a harmonic map is a stationary point of the Dirichlet energy over the set of vector fields between two Riemannian manifolds [53]. This is a classical subject in geometry, and we will follow the modern perspective from numerical analysis laid out in [24, Chap. 7], which formulates the problem in Sobolev and Lebesgue spaces and focuses on taking a manifold to a unit sphere.

Computing a harmonic map  $u$  between a domain  $\Omega \subset \mathbb{R}^n$  and the unit sphere  $\mathbb{S}^{m-1} \subset \mathbb{R}^m$ ,  $m \geq 2$ , requires minimizing the Dirichlet energy  $J$ , as defined in (3.1) with  $f \equiv 0$ , over the *nonconvex* feasible set

$$(5.2) \quad K = \{u \in H^1(\Omega; \mathbb{R}^m) \mid |u| = 1 \text{ a.e. in } \Omega \text{ and } u|_{\partial\Omega} = g\}.$$

Here, the boundary data  $g \in L^2(\partial\Omega; \mathbb{R}^m)$  must admit an  $H^1$ -extension  $u_g$  into the domain  $\Omega$  such that  $|u_g| = 1$ . Otherwise,  $K$  is clearly empty.

We choose to globalize the constraint before discretizing by adding a penalty term to  $J(u)$  that vanishes on the feasible set (5.2). This results in using the penalized objective function

$$(5.3) \quad J_\gamma(u) = \frac{1}{2} \int_{\Omega} |\nabla u|^2 \, dx + \frac{\gamma}{4} \int_{\Omega} (|u|^2 - 1)^2 \, dx,$$

where  $\gamma > 0$  is a tunable parameter. Since  $J(u) = J_\gamma(u)$  for all  $u \in K$ , and we still seek to enforce this constraint, the penalty term does not affect the set of solutions to the original minimization problem  $\min_{u \in K} J(u)$ . Indeed, we emphasize that the penalty term is not used to enforce the constraint but rather to aid the convergence of the LVPP scheme. We then arrive at the following sequence of LVPP subproblems: for some  $\psi^0 \in L^\infty(\Omega, \mathbb{R}^m)$ , find  $(u^k, \psi^k) \in H_g^1(\Omega; \mathbb{R}^m) \times L^\infty(\Omega, \mathbb{R}^m)$  such that

$$(5.4a) \quad \alpha_k(\nabla u^k, \nabla v) + \gamma(|u^k|^2 - 1)u^k, v + (\psi^k, v) = (\psi^{k-1}, v),$$

$$(5.4b) \quad (u^k, w) - (\psi^k/|\psi^k|, w) = 0,$$

for all  $(v, w) \in H_0^1(\Omega; \mathbb{R}^m) \times L^\infty(\Omega, \mathbb{R}^m)$ .

We further modify (5.4) before solving for  $u^k$  and  $\psi^k$  in practice. To this end, notice that the nonlinear term  $\psi^k \mapsto \psi^k/|\psi^k|$  in (5.4b) is invariant under pointwise rescalings of  $\psi^k$  and non-differentiable at  $\psi^k = 0$ . We account for these degeneracies by seeking to fix the magnitude  $|\psi^k(x)| = 1$  at a.e. point  $x \in \Omega$ . This change does not affect the constraint  $|u^k| = 1$  enforced by (5.4b). However, it results in the convenient identity  $u^k = \psi^k$  between the primal and latent variables. Using this identity to rewrite the second term in (5.4a) delivers the more stable reformulation

$$(5.5a) \quad \alpha_k(\nabla u^k, \nabla v) + \gamma(|\psi^k|^2 - 1)u^k, v + (\psi^k, v) = (\psi^{k-1}, v),$$

$$(5.5b) \quad (u^k, w) - (\psi^k/|\psi^k|, w) = 0,$$

that we use in the example problem below.

We solve this problem for  $\Omega = (0, 1)$  and  $m = 3$ , with results depicted in Figure 10. This setting is equivalent to computing geodesics on a sphere. In our implementation, we divide the interval  $\Omega$  into 1000 equally-spaced cells and then discretize (5.5) with continuous piecewise-quadratic finite elements for the  $u$ -variable and piecewise-linear

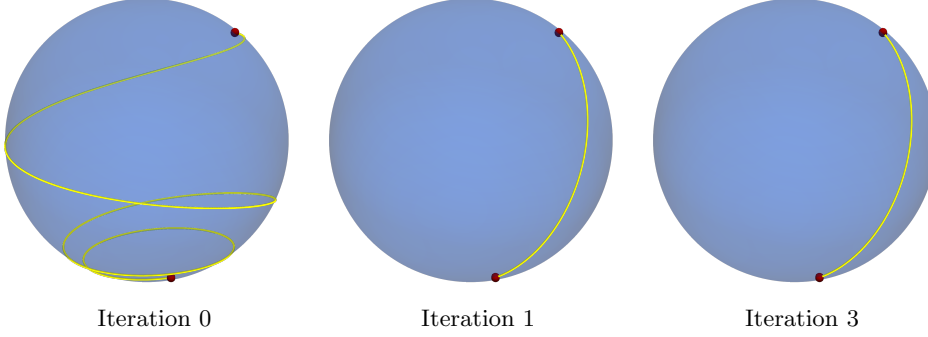


Fig. 10: Example 9. Geodesics on a sphere. From initial guess to optimized solution. Iteration 0 corresponds to the initial guess. The red dots correspond to the boundary conditions in (5.2) for  $\Omega = (0, 1)$ .

finite elements for the  $\psi$ -variable. The proximal step  $\alpha_k = 1$  is fixed for all iterations, and the penalty parameter  $\gamma$  is set to  $10^5$ . The initial condition  $\psi_h^0$  is the Lagrange interpolant of the function depicted by the yellow curve at iteration 0 in Figure 10. The endpoints of this curve (red dots) define the boundary conditions on  $u$ . The solver took three proximal steps, where the first step required 41 Newton iterations, the second two iterations, and the final step only one iteration. The absolute and relative tolerances were fixed at  $10^{-9}$  for Newton and  $10^{-8}$  for LVPP. We plot the iteration history in Figure 10. We note that the change in primal variable after the first step is less than  $10^{-7}$ .

**5.2. Example 10: Linear equality constraints.** For the sake of illustration, we demonstrate here the connection between the classical theory of saddle-point problems for linear subspace constraints [32] and the LVPP method. Moreover, we show that the LVPP approach to linear equality constraints converges in one iteration when applied to minimizing a quadratic objective function, an appealing property it shares with the Newton method [141]. The setting is abstract and general, but we do not seek maximal generality out of an effort to ease understanding.

Let  $V$  and  $W$  be real separable Hilbert spaces, with  $W$  continuously embedded in  $(L^2(\Omega))^m$ , and let  $B: V \rightarrow W$  be a bounded, surjective ( $\text{im } B = W$ ) linear operator. We define

$$(5.6) \quad K = \ker B = \{v \in V \mid Bv = 0\},$$

and consider optimizing a quadratic functional over  $K$ ,

$$(5.7) \quad J(v) = \frac{1}{2}a(v, v) - F(v),$$

where  $a: V \times V \rightarrow \mathbb{R}$  is a continuous, symmetric, coercive bilinear form, and  $F \in V'$ . In this case, the associated optimality conditions are well-known [32, Theorem 4.2.1], and reduce to the following variational problem: find  $u \in V$  and  $\lambda \in W$  such that

$$(5.8a) \quad a(u, v) + (\lambda, Bv) = F(v),$$

$$(5.8b) \quad (Bu, w) = 0,$$

for all  $v \in V$  and  $w \in W$ . For example, taking  $V = (H_0^1(\Omega))^d$ ,  $W = L_0^2(\Omega) := \{v \in L^2(\Omega) \mid \int_{\Omega} v \, dx = 0\}$ ,  $a(u, v) = (\nabla u, \nabla v)$ ,  $Bv = -\nabla \cdot v$  (the negative divergence

operator), and  $F(v) = (f, v)$  for a forcing function  $f \in (L^2(\Omega))^d$ , we get the Stokes equations [29] for unknown velocity  $u \in (H_0^1(\Omega))^d$  and pressure  $p \in L_0^2(\Omega)$ :

$$(5.9a) \quad (\nabla u, \nabla v) - (p, \nabla \cdot v) = (f, v),$$

$$(5.9b) \quad (\nabla \cdot u, q) = 0,$$

for all  $v \in (H_0^1(\Omega))^d$  and  $q \in L_0^2(\Omega)$ .

Upon setting  $C = \{0\}$  and  $\Omega_d = \Omega$ , the linear subspace  $K$  in (5.6) fits into the abstract setting (2.1). However, there is no Legendre function for  $C$  since this convex set has only a single point. As a remedy, we proceed by considering the closed unit ball centered at  $0 \in \mathbb{R}^m$ , denoted  $S(0, 1) = \{a \in \mathbb{R}^m \mid |x| \leq 1\}$ , with the Hellinger entropy  $R: S(0, 1) \rightarrow [-1, 0]$ ,  $a \mapsto -\sqrt{1 - |a|^2}$ . Given  $0 < \epsilon < 1$ , we define  $R_\epsilon = \epsilon R \circ (\epsilon^{-1} \text{id})$ , noting that  $\text{dom } R_\epsilon = S(0, \epsilon)$ .

The first LVPP subproblem that arises from minimizing  $J(v)$  in (5.7) over the feasible set

$$K_\epsilon = \{v \in V \mid Bv(x) \in S(0, \epsilon) \text{ for almost all } x \in \Omega\},$$

is as follows: for fixed  $\psi^0 \in W$ , find  $u_\epsilon \in V$  and  $\psi_\epsilon \in W$  such that

$$(5.10a) \quad \alpha_1 a(u_\epsilon, v) + (\psi_\epsilon, Bv) = \alpha_1 F(v) + (\psi^0, Bv),$$

$$(5.10b) \quad (Bu_\epsilon, w) - \epsilon(\nabla R^*(\psi_\epsilon), w) = 0,$$

for all  $v \in V$  and  $q \in W$ . Letting  $\epsilon$  pass to zero from above, we derive a saddle-point problem similar to (5.8). In particular, we can show that  $u_\epsilon \rightharpoonup \bar{u}$  weakly in  $V$  and  $\psi_\epsilon \rightharpoonup \bar{\psi}$  weakly in  $W$ , where  $\bar{u} \in V$  and  $\bar{\psi} \in W$  solve

$$(5.11a) \quad \alpha_1 a(\bar{u}, v) + (\bar{\psi}, Bv) = \alpha_1 F(v) + (\psi^0, Bv),$$

$$(5.11b) \quad (B\bar{u}, w) = 0,$$

for all  $v \in V$  and  $q \in W$ . Taking  $u = \bar{u}$  and  $\lambda = \alpha_1^{-1}(\bar{\psi} - \psi^0)$ , we arrive back at (5.8), which also ensures well-posedness of (5.11). We conclude that the latent variable approach always converges in one iteration and is equivalent to the standard Lagrange multiplier mixed method (5.8) for this class of problems. Rigorous details are provided in Appendix A for the interested reader.

**6. Applications to fully-nonlinear PDEs.** In addition to the applications demonstrated above, the LVPP methodology has a remarkable connection to certain fully-nonlinear PDEs. In Subsection 6.1, we first illustrate how LVPP leads to new mixed forms for first-order nonlinear PDEs. We provide computational evidence of the utility of such an approach by solving the eikonal equation. We then close the section by deriving a new geometric formulation of the classical Monge–Ampère equation by using matrix-valued latent variables and the matrix exponential function.

**6.1. Example 11: The eikonal equation.** Many nonlinear first-order PDEs have the following form [46]:

$$(6.1) \quad \text{find } u : \Omega \rightarrow \mathbb{R} \text{ such that } F(x, u, \nabla u) = 0 \text{ in } \Omega \text{ and } u = g \text{ on } \partial\Omega.$$

Generally, these equations lack a divergence structure, so one cannot integrate by parts to arrive at the correct notion of a weak solution. Instead, for suitable  $F$ , we opt for the concept of a viscosity solution introduced by Crandall and Lions [94, 45].

Viscosity solutions are directly linked to constrained optimization; see, e.g., [140, Proof of Thm. 1, Thm. 2]. Specifically, the viscosity solution of (6.1) minimizes

$$(6.2a) \quad J(u) = - \int_{\Omega} u \, dx$$

over the feasible set

$$(6.2b) \quad K = \{u \in W^{1,\infty}(\Omega) \mid F(x, u, \nabla u) \leq 0 \text{ f.a.e. } x \text{ in } \Omega \text{ and } u|_{\partial\Omega} = g\}.$$

Putting this feasible set  $K$  into our framework for general mappings  $F$  requires a generalization of (2.1) that would significantly complicate the paper. However, there are many interesting examples that we can immediately consider. For instance, upon defining  $F(x, u, \nabla u) = |\nabla u| - 1$  and taking  $g \equiv 0$ , the minimizer of (6.2) is the viscosity solution of the classical eikonal equation [46, 1.1.2],

$$(6.3) \quad |\nabla u| = 1 \text{ in } \Omega \text{ and } u = 0 \text{ on } \partial\Omega.$$

To obtain (6.2b) from (2.1) for this problem, we need only set  $V = H_0^1(\Omega)$ ,  $B = \nabla$ ,  $C$  to be the Euclidean ball of radius 1, and  $\Omega_d = \Omega$ .

The two most well-known methods for solving the eikonal equation are the fast marching [107, 122] and the fast sweeping [143, 142] methods. They are both finite difference-based schemes that trace back to Dijkstra's algorithm [50]. Both methods require specialized data structures that present a barrier to their integration into many of the high-order finite element codes used by the scientific computing community. On the other hand, the LVPP-based approach derived below is immediately compatible with such codes as it involves a Galerkin discretization with widely available finite elements.

Selecting the Hellinger entropy (4.2) with  $\phi \equiv 1$  and following the general framework for gradient-constrained problems described in Subsection 4.1, we deduce that minimizing (6.2a) over the feasible set (6.2b) leads to the following sequence of LVPP subproblems: for  $\psi^0 = 0$ , find  $(u^k, \psi^k) \in H_0^1(\Omega) \times L^2(\Omega, \mathbb{R}^n)$  satisfying

$$(6.4a) \quad (\psi^k, \nabla v) = \alpha_k(1, v) + (\psi^{k-1}, \nabla v),$$

$$(6.4b) \quad (\nabla u^k, w) - \left( \frac{\psi^k}{\sqrt{1 + |\psi^k|^2}}, w \right) = 0,$$

for all  $(v, w) \in H_0^1(\Omega) \times L^2(\Omega, \mathbb{R}^n)$ . Each of these subproblems may be seen as a nonlinear Darcy flow model (cf. [55, Chapter 51]), which we highlight by integrating each of the differential terms by parts and swapping the order of the equations. In particular, these operations require a change to the functional setting, revealing a new sequence of subproblems: for  $\psi^0 = 0$ , find  $(u^k, \psi^k) \in L^2(\Omega) \times H(\text{div}, \Omega)$  satisfying

$$(6.5a) \quad \left( \frac{\psi^k}{\sqrt{1 + |\psi^k|^2}}, w \right) + (u^k, \nabla \cdot w) = 0,$$

$$(6.5b) \quad (\nabla \cdot \psi^k, v) = (\nabla \cdot \psi^{k-1}, v) - \alpha_k(1, v),$$

for all  $(v, w) \in L^2(\Omega) \times H(\text{div}, \Omega)$ . We find that (6.5) admits the same popular finite element discretization used for that model.

We solved (6.5) on three different domains with the computed solutions presented in Figure 11: a two-dimensional star-shaped domain, a solid (three-dimensional)

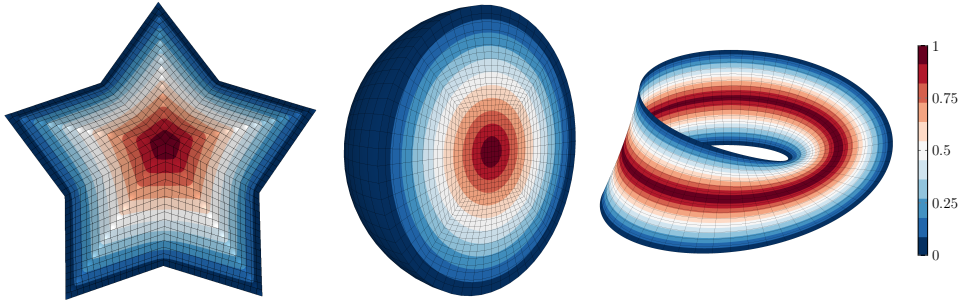


Fig. 11: Example 11. Viscosity solutions of the eikonal equation on a star-shaped domain (left), sphere (middle), and Möbius strip (right).

sphere, and a Möbius strip. To compare the results, we rescaled each domain so that the maximum, taken over all points in the domain, of the shortest distance to the domain boundary would be one. On the star-shaped domain and the sphere, we replaced  $L^2(\Omega)$  in (6.5) with a first-order discontinuous piecewise polynomial space and  $H(\text{div}, \Omega)$  with second-order Raviart–Thomas polynomial space, as this is the standard choice for Darcy flow problems. Showcasing additional flexibility in the discretization choices, we used a continuous piecewise polynomial discretization of Taylor–Hood-type inspired by [83] for the Möbius strip example. In particular, we used second-order Lagrange elements to approximate  $\psi^k$  and first-order Lagrange elements for  $u^k$ . We then set  $\alpha_k = 10 \cdot \min\{2^k, 5\}$  and solved each discretized subproblem with a damped Newton method. In each case, the solver took three Newton steps on the first subproblem ( $k = 1$ ) but only one Newton step for each subsequent subproblem ( $k > 1$ ). We stopped the solver once  $\|u^k - u^{k-1}\|_{L^2(\Omega)} < 10^{-4}$ , which always occurred in under ten iterations.

The setting above easily extends to solving other related problems. Indeed, selecting the general Hellinger entropy given in (4.2) results in multiplying the nonlinear function in (6.5a) by  $\phi$ , and allows one to treat the general eikonal equation,  $|\nabla u| = \phi$ . Alternatively, generalizing the objective function to  $J(u) = -\int_{\Omega} u f \, dx$  and minimizing it over the feasible set  $K = \{u \in H_0^1(\Omega) \mid |\nabla u| \leq 1 \text{ a.e. } x \text{ in } \Omega\}$  allows one to characterize the  $p \rightarrow \infty$  limit of solutions to the  $p$ -Laplace equation with  $f \in C(\bar{\Omega})$  [80]:

$$-\Delta_p u = f \text{ in } \Omega \quad \text{and} \quad u = 0 \text{ on } \partial\Omega.$$

To arrive at an algorithm to solve this problem, we need only to replace the right-most term in (6.5b) by  $-\alpha_k(f, v)$ .

**6.2. Example 12: The Monge–Ampère equation.** One can also define viscosity solutions to problem (6.1) if  $F$  depends on the Hessian  $\nabla^2 u$  [46, 56, 66]. Thus, the innovations above raise the question of whether our techniques can also be used to solve fully nonlinear *second-order* PDEs. We choose to provide a partial answer to this question by considering the celebrated Monge–Ampère equation, in which  $F(x, u, \nabla u, \nabla^2 u) = \det(\nabla^2 u) - \rho$ . More specifically, given uniformly positive functions  $\rho \in C(\bar{\Omega})$  and  $g \in C^3(\bar{\Omega})$  defined over a smooth, bounded, and uniformly convex domain  $\Omega \subset \mathbb{R}^n$ , we seek the unique convex function  $u \in H^2(\Omega) \cap H_g^1(\Omega)$  satisfying

$$(6.6) \quad \det(\nabla^2 u) = \rho \text{ in } \Omega, \quad u = g \text{ on } \partial\Omega.$$

We refer to [40, 120] for existence and regularity theory in this setting.

Although (6.6) is related to optimal transport [119], that connection to optimization does not yield an immediate insight into our approach. Instead, we focus on the fact that the set of feasible solutions,

$$K = \{u \in H^2(\Omega) \cap H_g^1(\Omega) \mid \nabla^2 u \succeq 0 \text{ a.e. in } \Omega\},$$

fits into the setting of (2.1) by taking  $V = H^2(\Omega) \cap H_g^1(\Omega)$ ,  $B = \nabla^2$ , and  $C$  equal to the set of all symmetric positive semidefinite  $n \times n$  matrices. We can now invoke a Legendre function to construct a structure-preserving reformulation of (6.6).

Consider the (unnormalized negative) von Neumann entropy [104, 14] for positive semidefinite symmetric matrices, defined by

$$R(a) = \text{tr}(a \ln a - a), \quad \text{with } \nabla R^*(a^*) = \exp a^*.$$

The convex geometry of  $K$  can be encoded by introducing a symmetric matrix-valued latent variable  $\psi$  via the equation  $Bu = \nabla R^*(\psi)$ ; i.e., we define

$$(6.7a) \quad \psi = \ln \nabla^2 u \quad \iff \quad \exp \psi = \nabla^2 u.$$

Finally, utilizing the identity  $\det(\exp \psi) = \exp(\text{tr } \psi)$  [71] and the original PDE (6.6), we see that  $\psi$  must satisfy the algebraic relation

$$(6.7b) \quad \text{tr } \psi = \ln \rho.$$

Together, (6.7a) and (6.7b) provide a reformulation of the Monge–Ampère equation that does not appear to have been explored in the literature; see [70, 60, 103] and the many references therein.

The following variational formulation of (6.7) is found by multiplying by smooth test functions and integrating over the domain  $\Omega$ : find  $u \in H^2(\Omega) \cap H_g^1(\Omega)$  and  $\psi \in L^\infty(\Omega; \mathbb{R}_{\text{sym}}^{n \times n})$  such that

$$(6.8a) \quad (\nabla^2 u, w) - (\exp \psi, w) = 0,$$

$$(6.8b) \quad (\text{tr } \psi, v) = (\ln \rho, v),$$

for all  $v \in H^2(\Omega) \cap H_0^1(\Omega)$  and  $w \in W$ . This formulation permits finite element discretizations with Argyris elements for  $u$  and  $v$ . However, due to the limited support for Argyris elements in most software, we suggest a first-order system discretization employing the most widely available types of elements. To this end, we introduce the optimal transport map  $T = \nabla u$  as a slack variable into the system of equations (6.8), leading to the following reformulation: find  $u \in H_g^1(\Omega)$ ,  $T \in H^1(\Omega, \mathbb{R}^n)$ , and  $\psi \in L^\infty(\Omega; \mathbb{R}_{\text{sym}}^{n \times n})$  such that

$$(6.9a) \quad (T, S) - (\nabla u, S) = 0,$$

$$(6.9b) \quad (\nabla T, w) - (\exp \psi, w) = 0,$$

$$(6.9c) \quad (\text{tr } \psi, v) = (\ln \rho, v),$$

for all  $v \in H_0^1(\Omega)$ ,  $S \in H^1(\Omega, \mathbb{R}^n)$ , and  $w \in W$ . We note that this is technically not an LVPP formulation, as there is no proximal loop. Likewise, its Galerkin finite element discretization should not be considered a proximal Galerkin method.

Our experiments indicate that formulation (6.9) permits high-order accurate, stable discretizations using degree- $p$  continuous elements for  $u$ , vector-valued degree- $(p+1)$  continuous elements for  $T$ , and matrix-valued degree- $p$  continuous elements

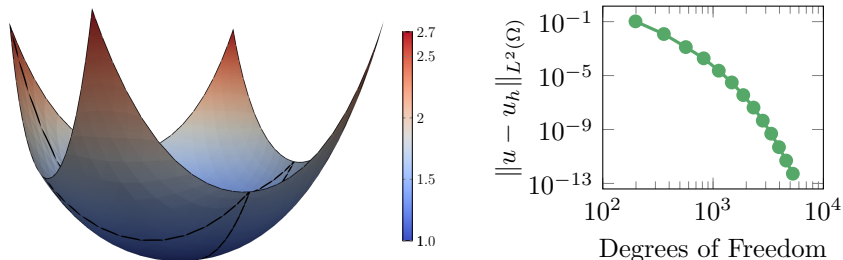


Fig. 12: Example 12. Exponential convergence of a manufactured solution to the Monge–Ampère equation on an eight-element mesh. Left: Computed solution with polynomial degree  $p = 14$ . Right: Degrees of freedom vs.  $L^2(\Omega)$ -error for polynomial degrees  $p = 2, 3, \dots, 14$ .

for  $\psi$ , if  $p \geq 2$ . Figure 12 showcases exponential convergence of the proposed method to a smooth manufactured solution  $u_{\text{man}}(x) = \exp(|x|^2/2)$  as the polynomial degree  $p$  is increased from 2 to 14. In this experiment, we set  $\Omega = (-1, 1)^2$ ,  $\rho = \det \nabla^2 u_{\text{man}}$  and  $g = u_{\text{man}}|_{\partial\Omega}$ . Starting from a linearization around  $\psi = 0$ , the resulting discretizations converged in no more than six Newton iterations on a uniform eight-element triangular mesh.

**7. Conclusion.** The LVPP algorithm provides a unifying mathematical framework for solving variational problems with pointwise inequality constraints. This framework is entirely separate from the quadratic penalty, interior point, active set, trust region, and augmented Lagrangian methods, which have been studied extensively over many decades. LVPP is derived at the level of the underlying function spaces, leaving it agnostic to the discretization strategy preferred for each application. In turn, the LVPP framework can be used to construct novel numerical methods—including, but not limited to, novel finite element, finite difference, and spectral methods—for a wide class of challenging problems.

We have selected twelve example problems and used the LVPP framework to derive state-of-the-art numerical methods for each of them. The first five examples include free-boundary and free-discontinuity problems, as well as quasi-variational inequalities with pointwise bound constraints. We find that LVPP delivers high-order, bound-preserving numerical methods for all five of these examples. The next three examples demonstrate how to apply LVPP to solve problems with gradient constraints, eigenvalue constraints, and multiple independent inequality constraints, respectively. Examples 9 and 10 then show how LVPP extends to treating linear and non-linear equality constraints. In the linear case (Example 10), we find that LVPP leads to a reformulation of the well-known saddle-point form of variational problems with linear equality constraints [32]. Lastly, the LVPP framework is used to derive new methods for computing viscosity solutions of first and second-order fully nonlinear PDEs. In each of these example problems, as well as every other problem we have attempted, LVPP or certain variants, see, e.g., [84, 87], have led to structure-preserving numerical methods that exhibit mesh-independence.

Each of the numerical methods in this paper requires further investigation. In most cases, our derivation of the particular LVPP saddle-point problem is formal and calls for a rigorous mathematical treatment in future work. Likewise, error analysis needs to be conducted on almost all of the derived methods to guarantee their convergence as the resolution of their discretization increases. We hope that other applied

mathematicians will join us in this task, and in applying LVPP to other problems with inequality constraints.

**Code availability.** In order to facilitate the broader adoption of this work by the community, we have implemented the derived methods across a range of popular open-source software libraries and prepared a suite of scripts to reproduce the numerical experiments. Scripts to generate all the examples are available at [52] and are archived on Zenodo [51]. We have implemented LVPP solvers in the finite element packages MFEM [11, 12], Firedrake [73], FEniCSx [23], and Gridap [17], and the spectral method package MultivariateOrthogonalPolynomials [105].

**Acknowledgements.** PEF was funded by the Engineering and Physical Sciences Research Council [grant numbers EP/R029423/1 and EP/W026163/1] and by the Donatio Universitatis Carolinae Chair “Mathematical modelling of multicomponent systems”. PEF would like to thank U. Zerbinati for help with Subsection 4.2. BK was supported in part by the U.S. Department of Energy Office of Science, Early Career Research Program under Award Number DE-SC0024335. IPAP was funded by the Deutsche Forschungsgemeinschaft (DFG, German Research Foundation) under Germany’s Excellence Strategy – The Berlin Mathematics Research Center MATH+ (EXC-2046/1, project ID: 390685689). For the purpose of open access, the authors have applied a CC BY public copyright licence to any author-accepted manuscript arising from this submission.

**Appendix A. Weak convergence in Subsection 5.2.** We complete the analysis showing that the solution of (5.10) weakly converges to the solution of (5.11) as  $\epsilon \downarrow 0$ . As we explicitly require using the coercivity and continuity constants to complete the argument, we note that  $a: V \times V \rightarrow \mathbb{R}$  being coercive means that there exists a positive number  $\beta > 0$  such that  $\beta \|v\|_V^2 \leq a(v, v)$  for all  $v \in V$ . Likewise, continuity means that there exists a number  $C$  such that  $a(u, v) \leq C \|u\|_V \|v\|_V$  for all  $u, v \in V$ .

Using  $u_\epsilon$  as a test function in (5.10a), we arrive at

$$(A.1) \quad \beta \|u_\epsilon\|_V^2 + \alpha_1^{-1} (\psi_\epsilon, Bu_\epsilon) \leq \|F\|_{V'} \|u_\epsilon\|_V + \alpha_1^{-1} \|B^* \psi^0\|_{V'} \|u_\epsilon\|_V,$$

where  $B^*: W \rightarrow V'$  denotes the  $L^2$ -adjoint of  $B$ . Next, we recall the identity  $\nabla R^*(0) = 0$  for the Hellinger entropy (4.2). Furthermore, note that  $R^*$  is a smooth convex function, and therefore, its gradient is a monotone operator. From these properties, we deduce the following inequality from (5.10a):

$$(A.2) \quad (\psi_\epsilon, Bu_\epsilon) = (\psi_\epsilon, \epsilon \nabla R^*(\psi_\epsilon)) = \epsilon (\psi_\epsilon - 0, \nabla R^*(\psi_\epsilon) - \nabla R^*(0)) \geq 0.$$

In turn, we find that  $u_\epsilon$  is bounded uniformly across  $\epsilon > 0$ ,

$$(A.3) \quad \beta \|u_\epsilon\|_V \leq \|F\|_{V'} + \alpha_1^{-1} \|B^* \psi^0\|_{V'}.$$

The uniform bound given above allows us to pass to the limit for a (positive) null sequence  $\epsilon_k \downarrow 0$ . Even without knowledge of the convergence properties of  $\psi_{\epsilon_k}$ , we can deduce that the sequence

$$\epsilon_k \nabla R^*(\psi_{\epsilon_k}) \rightarrow 0 \text{ in } L^\infty(\Omega)$$

since the nonlinearity remains bounded in the bounded set  $S(0, 1)$ . By reflexivity, there exists a subsequence  $\{\epsilon_{k_l}\}$  along which  $u_{\epsilon_{k_l}}$  converges weakly in  $V$  to some

$\bar{u}$ . In particular, we may conclude that  $B\bar{u} = 0$ . Next, we invoke the closed range theorem and the surjectivity of  $B: V \rightarrow W$  to establish the existence of a constant  $c > 0$ , independent of  $\epsilon$ , such that

$$c\|\psi_\epsilon\|_W \leq \|B^*\psi_\epsilon\|_{V'} = \sup_{v \in V} \frac{|(\psi_\epsilon, Bv)|}{\|v\|_V} \leq \alpha_1\|F\|_{V'} + \|B^*\psi^0\|_{V'} + \alpha_1 C\|u_\epsilon\|_V.$$

This and (A.3) shows that  $\psi_\epsilon$  is bounded uniformly across  $\epsilon > 0$ . By reflexivity of  $W$ , there exists a weak accumulation point  $\bar{\psi} \in W$  of  $\psi_{\epsilon_k}$  for any sequence  $\epsilon_k \downarrow 0$ . This implies that  $(\psi_\epsilon - \psi^0)/\alpha_1$  will (weakly) converge along an appropriate subsequence to  $(\bar{\psi} - \psi^0)/\alpha_1$ . As observed above, we can take  $\bar{u} = u$  and  $\lambda = (\bar{\psi} - \psi^0)/\alpha_1$  in (5.8). Since  $u$  and  $\lambda$  are unique it follows from the Fréchet-Urysohn property that the full sequence converges weakly, i.e.,  $u_\epsilon \rightharpoonup u$  in  $V$  and  $(\psi_\epsilon - \psi^0)/\alpha_1 \rightharpoonup \lambda$  in  $W$  as  $\epsilon \downarrow 0$ , as necessary.

#### REFERENCES

- [1] L. ADAM, M. HINTERMÜLLER, D. PESCHKA, AND T. M. SUROWIEC, *Optimization of a multi-physics problem in semiconductor laser design*, SIAM Journal on Applied Mathematics, 79 (2019), p. 257–283, <https://doi.org/10.1137/18m1179183>.
- [2] L. ADAM, M. HINTERMÜLLER, AND T. M. SUROWIEC, *A semismooth Newton method with analytical path-following for the  $H^1$ -projection onto the Gibbs simplex*, IMA Journal of Numerical Analysis, 39 (2018), pp. 1276–1295, <https://doi.org/10.1093/imanum/dry034>.
- [3] R. AGARWAL AND D. O'REGAN, *Nonlinear generalized quasi-variational inequalities: A fixed point approach*, Mathematical Inequalities & Applications, 6 (2003), pp. 133–143, <https://doi.org/10.7153/mia-06-13>.
- [4] E. L. ALLGOWER, K. BÖHMER, F. POTRA, AND W. RHEINBOLDT, *A mesh-independence principle for operator equations and their discretizations*, SIAM Journal on Numerical Analysis, 23 (1986), pp. 160–169, <https://doi.org/10.1137/0723011>.
- [5] M. S. ALNÆS, A. LOGG, K. B. ØLGAARD, M. E. ROGNES, AND G. N. WELLS, *Unified Form Language: a domain-specific language for weak formulations of partial differential equations*, ACM Transactions on Mathematical Software, 40 (2014), pp. 9:1–9:37, <https://doi.org/10.1145/2566630>.
- [6] A. ALPHONSE, C. CHRISTOF, M. HINTERMÜLLER, AND I. P. A. PAPADOPOULOS, *A globalized inexact semismooth Newton method for nonsmooth fixed-point equations involving variational inequalities*, arXiv preprint arXiv:2409.19637, (2024), <https://doi.org/10.48550/arXiv.2409.19637>.
- [7] A. ALPHONSE, M. HINTERMÜLLER, AND C. N. RAUTENBERG, *Directional differentiability for elliptic quasi-variational inequalities of obstacle type*, Calculus of Variations and Partial Differential Equations, 58 (2019), p. 39, <https://doi.org/10.1007/s00526-018-1473-0>.
- [8] A. ALPHONSE, M. HINTERMÜLLER, AND C. N. RAUTENBERG, *Recent trends and views on elliptic quasi-variational inequalities*, Springer, 2019, [https://doi.org/10.1007/978-3-030-33116-0\\_1](https://doi.org/10.1007/978-3-030-33116-0_1).
- [9] S.-I. AMARI, *Information Geometry and Its Applications*, Springer Japan, 2016, <https://doi.org/10.1007/978-4-431-55978-8>.
- [10] L. AMBROSIO AND V. M. TORTORELLI, *Approximation of functional depending on jumps by elliptic functional via  $t$ -convergence*, Communications on Pure and Applied Mathematics, 43 (1990), p. 999–1036, <https://doi.org/10.1002/cpa.3160430805>.
- [11] R. ANDERSON, J. ANDREJ, A. BARKER, J. BRAMWELL, J.-S. CAMIER, J. CERVENY, V. DOBREV, Y. DUDOUIT, A. FISHER, T. KOLEV, W. PAZNER, M. STOWELL, V. TOMOV, I. AKKERMAN, J. DAHM, D. MEDINA, AND S. ZAMPINI, *MFEM: A modular finite element methods library*, Computers & Mathematics with Applications, 81 (2021), pp. 42–74, <https://doi.org/10.1016/j.camwa.2020.06.009>.
- [12] J. ANDREJ, N. ATALLAH, J.-P. BÄCKER, J.-S. CAMIER, D. COPELAND, V. DOBREV, Y. DUDOUIT, T. DUSWALD, B. KEITH, D. KIM, ET AL., *High-performance finite elements with MFEM*, The International Journal of High Performance Computing Applications, 38 (2024), pp. 447–467.
- [13] H. ANTIL, R. ARNDT, C. N. RAUTENBERG, AND D. VERMA, *Nondiffusive variational problems with distributional and weak gradient constraints*, Advances in Nonlinear Analysis, 11

- (2022), pp. 1466–1495, <https://doi.org/doi:10.1515/anona-2022-0227>.
- [14] H. ARAKI AND E. H. LIEB, *Entropy inequalities*, Communications in Mathematical Physics, 18 (1970), p. 160–170, <https://doi.org/10.1007/bf01646092>.
- [15] D. N. ARNOLD, *Finite element exterior calculus*, Society for Industrial and Applied Mathematics, 2018, <https://doi.org/10.1137/1.9781611975543>.
- [16] J. AUBIN, *Mathematical Methods of Game and Economic Theory*, Dover books on mathematics, Dover Publications, 2007.
- [17] S. BADIA AND F. VERDUGO, *Gridap: An extensible finite element toolbox in Julia*, Journal of Open Source Software, 5 (2020), p. 2520, <https://doi.org/10.21105/joss.02520>.
- [18] C. BAIOCCHI AND A. CAPELO, *Variational and Quasivariational Inequalities*, A Wiley-Interscience Publication, John Wiley & Sons, Inc., New York, 1984.
- [19] S. BALAY, S. ABHYANKAR, M. F. ADAMS, S. BENSON, J. BROWN, P. BRUNE, ET AL., *PETSc/TAO users manual*, Tech. Report ANL-21/39 - Revision 3.21, Argonne National Laboratory, 2024, <https://doi.org/10.2172/2205494>.
- [20] J. M. BALL, *Mathematics and liquid crystals*, Molecular Crystals and Liquid Crystals, 647 (2017), pp. 1–27, <https://doi.org/10.1080/15421406.2017.1289425>.
- [21] J. M. BALL AND A. MAJUMDAR, *Nematic liquid crystals: from Maier–Saupe to a continuum theory*, Molecular Crystals and Liquid Crystals, 525 (2010), pp. 1–11, <https://doi.org/10.1080/15421401003795555>.
- [22] L. BANZ AND A. SCHRÖDER, *Biorthogonal basis functions in hp-adaptive FEM for elliptic obstacle problems*, Computers & Mathematics with Applications, 70 (2015), pp. 1721–1742, <https://doi.org/10.1016/j.camwa.2015.07.010>.
- [23] I. A. BARATTA, J. P. DEAN, J. S. DOKKEN, M. HABERA, J. S. HALE, C. N. RICHARDSON, M. E. ROGNES, M. W. SCROGGS, N. SIME, AND G. N. WELLS, *DOLFINx: The next generation FEniCS problem solving environment*. Unpublished, 2023, <https://doi.org/10.5281/zenodo.10447666>.
- [24] S. BARTELS, *Numerical Methods for Nonlinear Partial Differential Equations*, Springer International Publishing, 2015, <https://doi.org/10.1007/978-3-319-13797-1>.
- [25] H. H. BAUSCHKE AND J. M. BORWEIN, *Legendre functions and the method of random Bregman projections*, Journal of convex analysis, 4 (1997), pp. 27–67.
- [26] S. J. BENSON AND T. S. MUNSON, *Flexible complementarity solvers for large-scale applications*, Optimization Methods and Software, 21 (2006), pp. 155–168, <https://doi.org/10.1080/10556780500065382>.
- [27] A. BENSOUSSAN AND J. L. LIONS, *Optimal impulse and continuous control: Method of nonlinear quasi-variational inequalities*, Trudy Matematicheskogo Instituta imeni V.A. Steklova, 134 (1975), pp. 5–22.
- [28] A. BENSOUSSAN AND J.-L. LIONS, *Impulse Control and Quasivariational Inequalities*, Gauthier-Villars, Montrouge; Heyden & Son, Inc., Philadelphia, PA, 1984.
- [29] C. BERNARDI, V. GIRAULT, F. HECHT, P.-A. RAVIART, AND B. RIVIÈRE, *Mathematics and Finite Element Discretizations of Incompressible Navier-Stokes Flows*, SIAM, 2024, <https://doi.org/10.1137/1.9781611978124>.
- [30] D. BERNSTEIN AND W. SO, *Some explicit formulas for the matrix exponential*, IEEE Transactions on Automatic Control, 38 (1993), pp. 1228–1232, <https://doi.org/10.1109/9.233156>.
- [31] L. BIEGLER, *Nonlinear Programming: Concepts, Algorithms, and Applications to Chemical Processes*, MOS-SIAM Series on Optimization, Society for Industrial and Applied Mathematics (SIAM, 3600 Market Street, Floor 6, Philadelphia, PA 19104), 2010, <https://doi.org/10.1137/1.9780898719383>.
- [32] D. BOFFI, F. BREZZI, AND M. FORTIN, *Mixed finite element methods and applications*, vol. 44, Springer, 2013, <https://doi.org/10.1007/978-3-540-78319-0>.
- [33] B. BOURDIN, G. FRANCFORT, AND J.-J. MARIGO, *Numerical experiments in revisited brittle fracture*, Journal of the Mechanics and Physics of Solids, 48 (2000), p. 797–826, [https://doi.org/10.1016/s0022-5096\(99\)00028-9](https://doi.org/10.1016/s0022-5096(99)00028-9).
- [34] L. BREGMAN, *The relaxation method of finding the common point of convex sets and its application to the solution of problems in convex programming*, USSR Computational Mathematics and Mathematical Physics, 7 (1967), pp. 200–217, [https://doi.org/10.1016/0041-5553\(67\)90040-7](https://doi.org/10.1016/0041-5553(67)90040-7).
- [35] H. BREZIS AND M. SIBONY, *Equivalence de deux inéquations variationnelles et applications*, Archive for Rational Mechanics and Analysis, 41 (1971), p. 254–265, <https://doi.org/10.1007/bf00250529>.
- [36] J. A. BRÜGGEMANN, *A class of elliptic obstacle-type quasi-variational inequalities: Theory and solution methods*, Humboldt-Universität zu Berlin, (2023), <https://doi.org/10.18452/27750>.

- [37] E. BUELER AND P. E. FARRELL, *A full approximation scheme multilevel method for nonlinear variational inequalities*, SIAM Journal on Scientific Computing, 46 (2024), pp. A2421–A2444, <https://doi.org/10.1137/23M1594200>.
- [38] S. BURKE, C. ORTNER, AND E. SÜLI, *An adaptive finite element approximation of a variational model of brittle fracture*, SIAM Journal on Numerical Analysis, 48 (2010), pp. 980–1012, <https://doi.org/10.1137/080741033>.
- [39] K. J. BURNS, G. M. VASIL, J. S. OISHI, D. LECOANET, AND B. P. BROWN, *Dedalus: A flexible framework for numerical simulations with spectral methods*, Physical Review Research, 2 (2020), p. 023068, <https://doi.org/10.1103/PhysRevResearch.2.023068>.
- [40] L. A. CAFFARELLI, *Interior  $W^{2,p}$  estimates for solutions of the Monge–Ampère equation*, The Annals of Mathematics, 131 (1990), p. 135, <https://doi.org/10.2307/1971510>.
- [41] E. CASAS AND L. A. FERNÁNDEZ, *Optimal control of semilinear elliptic equations with pointwise constraints on the gradient of the state*, Applied Mathematics & Optimization, 27 (1993), p. 35–56, <https://doi.org/10.1007/bf01182597>.
- [42] G. CHEN AND M. TEBoulLE, *Convergence analysis of a proximal-like minimization algorithm using Bregman functions*, SIAM Journal on Optimization, 3 (1993), pp. 538–543, <https://doi.org/10.1137/0803026>.
- [43] H.-W. CHENG AND S. S.-T. YAU, *More explicit formulas for the matrix exponential*, Linear Algebra and its Applications, 262 (1997), pp. 131–163, [https://doi.org/10.1016/S0024-3795\(97\)80028-6](https://doi.org/10.1016/S0024-3795(97)80028-6).
- [44] F. H. CLARKE, *Optimization and Nonsmooth Analysis*, Society for Industrial and Applied Mathematics, Jan. 1990, <https://doi.org/10.1137/1.9781611971309>.
- [45] M. G. CRANDALL AND P.-L. LIONS, *Viscosity solutions of Hamilton–Jacobi equations*, Transactions of the American Mathematical Society, 277 (1983), p. 1–42, <https://doi.org/10.1090/S0002-9947-1983-0690039-8>.
- [46] B. DACOROGNA AND P. MARCELLINI, *Implicit partial differential equations*, Progress in Nonlinear Differential Equations and Their Applications, Birkhäuser, Cambridge, MA, 1999 ed., Aug. 1999, <https://doi.org/10.1007/978-1-4612-1562-2>.
- [47] G. DAL MASO, *An Introduction to  $\Gamma$ -Convergence*, Birkhäuser Boston, 1993, <https://doi.org/10.1007/978-1-4612-0327-8>.
- [48] P. G. DE GENNES AND J. PROST, *The physics of liquid crystals*, International Series of Monographs on Physics, Oxford University Press, 2 ed., 1995.
- [49] J. P. DEAN, *Mathematical and computational aspects of solving mixed-domain problems using the finite element method*, PhD thesis, University of Cambridge, Cambridge, UK, 2024, <https://doi.org/10.17863/CAM.108292>.
- [50] E. W. DIJKSTRA, *A note on two problems in connexion with graphs*, Numerische Mathematik, 1 (1959), p. 269–271, <https://doi.org/10.1007/bf01386390>.
- [51] J. S. DOKKEN, P. E. FARRELL, B. KEITH, I. P. PAPADOPOULOS, AND T. M. SUROWIEC, *The latent variable proximal point algorithm for variational problems with inequality constraints*, Mar. 2025, <https://doi.org/10.5281/zenodo.14918044>.
- [52] J. S. DOKKEN, P. E. FARRELL, B. KEITH, I. P. A. PAPADOPOULOS, AND T. M. SUROWIEC, *ProximalGalerkin*, 2025, <https://github.com/METHODS-Group/ProximalGalerkin>.
- [53] J. EELLS AND J. H. SAMPSON, *Harmonic mappings of Riemannian manifolds*, American Journal of Mathematics, 86 (1964), p. 109, <https://doi.org/10.2307/2373037>.
- [54] C. ELLIOTT, D. FRENCH, AND F. MILNER, *A second order splitting method for the Cahn–Hilliard equation.*, Numerische Mathematik, 54 (1989), pp. 575–590, <https://doi.org/10.1007/BF01396363>.
- [55] A. ERN AND J.-L. GUERMOND, *Finite Elements II: Galerkin Approximation, Elliptic and Mixed PDEs*, Springer International Publishing, Cham, 2021, [https://doi.org/10.1007/978-3-030-56923-5\\_51](https://doi.org/10.1007/978-3-030-56923-5_51).
- [56] L. EVANS, *Partial Differential Equations*, American Mathematical Society, Mar. 2010, <https://doi.org/10.1090/gsm/019>.
- [57] J. R. FANCHI, *Principles of applied reservoir simulation*, Gulf Publishing, Oxford, England, 3 ed., Dec. 2005, <https://doi.org/10.1016/B978-0-7506-7933-6.X5000-4>.
- [58] P. E. FARRELL, M. CROCI, AND T. M. SUROWIEC, *Deflation for semismooth equations*, Optimization Methods and Software, 35 (2019), pp. 1248–1271, <https://doi.org/10.1080/10556788.2019.1613655>.
- [59] G. FICHERA, *Sul problema elastostatico di Signorini con ambigue condizioni al contorno*, Atti della Accademia Nazionale dei Lincei, Classe di Scienze Fisiche, Matematiche e Naturali, 34 (1963), pp. 138–142.
- [60] A. FIGALLI, *The Monge–Ampère Equation and Its Applications*, EMS Press, Jan. 2017, <https://doi.org/10.4171/170>, <http://dx.doi.org/10.4171/170>.

- [61] G. FRANCFORT AND J.-J. MARIGO, *Revisiting brittle fracture as an energy minimization problem*, Journal of the Mechanics and Physics of Solids, 46 (1998), p. 1319–1342, [https://doi.org/10.1016/s0022-5096\(98\)00034-9](https://doi.org/10.1016/s0022-5096(98)00034-9).
- [62] G. FU, B. KEITH, AND R. MASRI, *A locally-conservative proximal Galerkin method for pointwise bound constraints*, arXiv preprint arXiv:2412.21039, (2024).
- [63] H. GARCKE, B. NESTLER, AND B. STOTH, *On anisotropic order parameter models for multiphase systems and their sharp interface limits*, Physica D: Nonlinear Phenomena, 115 (1998), p. 87–108, [https://doi.org/10.1016/s0167-2789\(97\)00227-3](https://doi.org/10.1016/s0167-2789(97)00227-3).
- [64] H. GARCKE, B. NESTLER, AND B. STOTH, *A multiphase field concept: Numerical simulations of moving phase boundaries and multiple junctions*, SIAM Journal on Applied Mathematics, 60 (1999), pp. 295–315, <https://doi.org/10.1137/S0036139998334895>.
- [65] T. GERASIMOV, U. RÖMER, J. VONDŘEJC, H. G. MATTHIES, AND L. DE LORENZIS, *Stochastic phase-field modeling of brittle fracture: computing multiple crack patterns and their probabilities*, Computer Methods in Applied Mechanics and Engineering, 372 (2020), p. 113353, <https://doi.org/10.1016/j.cma.2020.113353>.
- [66] D. GILBARG AND N. S. TRUDINGER, *Elliptic partial differential equations of second order*, vol. 224, Springer, 1977.
- [67] R. GLOWINSKI, J.-L. LIONS, AND R. TRÉMOLIÈRES, *Numerical analysis of variational inequalities*, Studies in Mathematics and Its Applications, North-Holland, May 2014.
- [68] N. I. M. GOULD, D. ORBAN, AND P. L. TOINT, *GALAHAD, a library of thread-safe Fortran 90 packages for large-scale nonlinear optimization*, ACM Transactions on Mathematical Software, 29 (2003), p. 353–372, <https://doi.org/10.1145/962437.962438>.
- [69] T. GUSTAFSSON, R. STENBERG, AND J. VIDEMAN, *On finite element formulations for the obstacle problem—mixed and stabilised methods*, Computational Methods in Applied Mathematics, 17 (2017), pp. 413–429, <https://doi.org/10.1515/cmam-2017-0011>.
- [70] C. E. GUTIÉRREZ, *The Monge-Ampère Equation*, Springer International Publishing, 2016, <https://doi.org/10.1007/978-3-319-43374-5>.
- [71] H. E. HABER, *Notes on the matrix exponential and logarithm*, Santa Cruz Institute for Particle Physics, University of California: Santa Cruz, CA, USA, (2018).
- [72] W. HACKBUSCH AND H. D. MITTELMANN, *On multi-grid methods for variational inequalities*, Numerische Mathematik, 42 (1983), pp. 65–76, <https://doi.org/10.1007/BF01400918>.
- [73] D. A. HAM, P. H. J. KELLY, L. MITCHELL, C. J. COTTER, R. C. KIRBY, K. SAGIYAMA, N. BOUZIANI, ET AL., *Firedrake User Manual*, Imperial College London and University of Oxford and Baylor University and University of Washington, first edition ed., 5 2023, <https://doi.org/10.25561/104839>.
- [74] M. HINTERMÜLLER, K. ITO, AND K. KUNISCH, *The primal-dual active set strategy as a semismooth Newton method*, SIAM Journal on Optimization, 13 (2002), pp. 865–888, <https://doi.org/10.1137/S1052623401383558>.
- [75] M. HINTERMÜLLER AND K. KUNISCH, *Feasible and noninterior path-following in constrained minimization with low multiplier regularity*, SIAM Journal on Control and Optimization, 45 (2006), pp. 1198–1221, <https://doi.org/10.1137/050637480>.
- [76] M. HINTERMÜLLER AND K. KUNISCH, *PDE-constrained optimization subject to pointwise constraints on the control, the state, and its derivative*, SIAM Journal on Optimization, 20 (2010), p. 1133–1156, <https://doi.org/10.1137/080737265>.
- [77] M. HINTERMÜLLER AND C. N. RAUTENBERG, *A sequential minimization technique for elliptic quasi-variational inequalities with gradient constraints*, SIAM Journal on Optimization, 22 (2012), p. 1224–1257, <https://doi.org/10.1137/110837048>.
- [78] M. HINTERMÜLLER AND K. KUNISCH, *Path-following methods for a class of constrained minimization problems in function space*, SIAM Journal on Optimization, 17 (2006), pp. 159–187, <https://doi.org/10.1137/040611598>.
- [79] R. H. HOPPE, *Multigrid algorithms for variational inequalities*, SIAM Journal on Numerical Analysis, 24 (1987), pp. 1046–1065, <https://doi.org/10.1137/0724069>.
- [80] H. ISHII AND P. LORETI, *Limits of solutions of p-Laplace equations as p goes to infinity and related variational problems*, SIAM Journal on Mathematical Analysis, 37 (2005), pp. 411–437, <https://doi.org/10.1137/S0036141004432827>.
- [81] P. JAILLET, D. LAMBERTON, AND B. LAPEYRE, *Variational inequalities and the pricing of American options*, Acta Applicandae Mathematicae, 21 (1990), pp. 263–289, <https://doi.org/10.1007/bf00047211>.
- [82] C. KANZOW AND D. STECK, *Quasi-variational inequalities in Banach spaces: Theory and augmented Lagrangian methods*, SIAM Journal on Optimization, 29 (2019), pp. 3174–3200, <https://doi.org/10.1137/18M1230475>.
- [83] T. KARPER, K.-A. MARDAL, AND R. WINTHER, *Unified finite element discretizations of cou-*

- pled Darcy–Stokes flow*, Numerical Methods for Partial Differential Equations: An International Journal, 25 (2009), pp. 311–326.
- [84] B. KEITH, D. KIM, B. S. LAZAROV, AND T. M. SUROWIEC, *Analysis of the SiMPL method for density-based topology optimization*, arXiv preprint arXiv:2409.19341, (2024). To appear in SIAM Journal on Optimization.
- [85] B. KEITH AND T. M. SUROWIEC, *Proximal Galerkin: A structure-preserving finite element method for pointwise bound constraints*, Foundations of Computational Mathematics, (2024), <https://doi.org/10.1007/s10208-024-09681-8>.
- [86] N. KIKUCHI AND J. T. ODEN, *Contact Problems in Elasticity*, Society for Industrial and Applied Mathematics, 1988, <https://doi.org/10.1137/1.9781611970845>.
- [87] D. KIM, B. S. LAZAROV, T. M. SUROWIEC, AND B. KEITH, *A simple introduction to the SiMPL method for density-based topology optimization*, arXiv preprint arXiv:2411.19421, (2024).
- [88] D. KINDERLEHRER AND G. STAMPACCHIA, *An Introduction to Variational Inequalities and Their Applications*, Society for Industrial and Applied Mathematics, 2000, <https://doi.org/10.1137/1.9780898719451>.
- [89] R. C. KIRBY, *Fast simplicial finite element algorithms using Bernstein polynomials*, Numerische Mathematik, 117 (2010), p. 631–652, <https://doi.org/10.1007/s00211-010-0327-2>.
- [90] R. KORNUBER, *Monotone multigrid methods for elliptic variational inequalities I*, Numerische Mathematik, 69 (1994), pp. 167–184, <https://doi.org/10.1007/BF03325426>.
- [91] S. KRALJ AND A. MAJUMDAR, *Order reconstruction patterns in nematic liquid crystal wells*, Proceedings of the Royal Society A, 470 (2014), p. 20140276, <https://doi.org/10.1098/rspa.2014.0276>.
- [92] M. KRUZÍK AND A. PROHL, *Recent developments in the modeling, analysis, and numerics of ferromagnetism*, SIAM Review, 48 (2006), p. 439–483, <https://doi.org/10.1137/s0036144504446187>.
- [93] L. LANDAU AND E. LIFSHTIZ, *On the theory of the dispersion of magnetic permeability in ferromagnetic bodies*, Phys. Z. Sowjetunion, 8 (1935), pp. 101–114.
- [94] P.-L. LIONS, *Generalized solutions of Hamilton–Jacobi equations*, Pitman Publishing, Harlow, England, 1982.
- [95] P.-L. LIONS AND B. PERTHAME, *Quasi-variational inequalities and ergodic impulse control*, SIAM Journal on Control and Optimization, 24 (1986), pp. 604–615, <https://doi.org/10.1137/0324036>.
- [96] U. MACKENROTH, *On some elliptic optimal control problems with state constraints*, Optimization, 17 (1986), p. 595–607, <https://doi.org/10.1080/02331938608843174>.
- [97] A. MAJUMDAR, *Equilibrium order parameters of nematic liquid crystals in the Landau–de Gennes theory*, European Journal of Applied Mathematics, 21 (2010), pp. 181–203, <https://doi.org/10.1017/s0956792509990210>.
- [98] L. MODICA, *The gradient theory of phase transitions and the minimal interface criterion*, Archive for Rational Mechanics and Analysis, 98 (1987), p. 123–142, <https://doi.org/10.1007/bf00251230>.
- [99] L. MODICA, *Gradient theory of phase transitions with boundary contact energy*, Annales de l’Institut Henri Poincaré C, Analyse non linéaire, 4 (1987), p. 487–512, [https://doi.org/10.1016/s0294-1449\(16\)30360-2](https://doi.org/10.1016/s0294-1449(16)30360-2).
- [100] U. MOSCO, *Implicit variational problems and quasi variational inequalities*, in Nonlinear operators and the calculus of variations (Summer School, Univ. Libre Bruxelles, Brussels, 1975), Lecture Notes in Math., Vol. 543, Springer, Berlin, 1976, pp. 83–156, <https://doi.org/10.1007/BFb0079943>.
- [101] D. MUMFORD AND J. SHAH, *Optimal approximations by piecewise smooth functions and associated variational problems*, Communications on Pure and Applied Mathematics, 42 (1989), p. 577–685, <https://doi.org/10.1002/cpa.3160420503>.
- [102] T. S. MUNSON, F. FACCHINEL, M. C. FERRIS, A. FISCHER, AND C. KANZOW, *The semismooth algorithm for large scale complementarity problems*, INFORMS Journal on Computing, 13 (2001), pp. 294–311, <https://doi.org/10.1287/ijoc.13.4.294.9734>.
- [103] M. NEILAN, A. J. SALGADO, AND W. ZHANG, *The Monge–Ampère equation*, Elsevier, 2020, p. 105–219, <https://doi.org/10.1016/bs.hna.2019.05.003>.
- [104] J. V. NEUMANN, *Thermodynamik quantenmechanischer Gesamtheiten*, Nachrichten von der Gesellschaft der Wissenschaften zu Göttingen, Mathematisch-Physikalische Klasse, 1927 (1927), pp. 273–291, <http://eudml.org/doc/59231>.
- [105] S. OLVER ET AL., *MultivariateOrthogonalPolynomials.jl*, 2024, <https://github.com/JuliaApproximation/MultivariateOrthogonalPolynomials.jl>.

- [106] S. OLVER AND A. TOWNSEND, *A fast and well-conditioned spectral method*, SIAM Review, 55 (2013), pp. 462–489, <https://doi.org/10.1137/120865458>.
- [107] S. OSHER AND J. A. SETHIAN, *Fronts propagating with curvature-dependent speed: Algorithms based on Hamilton–Jacobi formulations*, Journal of Computational Physics, 79 (1988), p. 12–49, [https://doi.org/10.1016/0021-9991\(88\)90002-2](https://doi.org/10.1016/0021-9991(88)90002-2).
- [108] I. P. A. PAPADOPOULOS, *Hierarchical proximal Galerkin: a fast hp-FEM solver for variational problems with pointwise inequality constraints*, 2024, <https://doi.org/10.48550/arXiv.2412.13733>.
- [109] I. P. A. PAPADOPOULOS, T. S. GUTLEB, R. M. SLEVINSKY, AND S. OLVER, *Building hierarchies of semiclassical Jacobi polynomials for spectral methods in annuli*, SIAM Journal on Scientific Computing, 46 (2024), pp. A3448–A3476, <https://doi.org/10.1137/23M160846X>.
- [110] L. PRIGOZHIN, *Sandpiles and river networks: Extended systems with nonlocal interactions*, Phys. Rev. E, 49 (1994), pp. 1161–1167, <https://doi.org/10.1103/PhysRevE.49.1161>.
- [111] L. PRIGOZHIN, *On the Bean critical-state model in superconductivity*, European Journal of Applied Mathematics, 7 (1996), p. 237–247, <https://doi.org/10.1017/S0956792500002333>.
- [112] L. PRIGOZHIN, *Variational model of sandpile growth*, European Journal of Applied Mathematics, 7 (1996), p. 225–235, <https://doi.org/10.1017/S0956792500002321>.
- [113] H. RISKEN, *The Fokker-Planck Equation: Methods of Solution and Applications*, Springer Berlin Heidelberg, 1996, <https://doi.org/10.1007/978-3-642-61544-3>.
- [114] M. ROBINSON, C. LUO, P. E. FARRELL, R. ERBAN, AND A. MAJUMDAR, *From molecular to continuum modelling of bistable liquid crystal devices.*, Liquid Crystals, 44 (2017), pp. 2267–2284, <https://doi.org/10.1080/02678292.2017.1290284>.
- [115] R. T. ROCKAFELLAR, *Conjugates and Legendre transforms of convex functions*, Canadian Journal of Mathematics, 19 (1967), pp. 200–205, <https://doi.org/10.4153/CJM-1967-012-4>.
- [116] R. T. ROCKAFELLAR, *Convex Analysis*, Princeton University Press, Princeton, 1970.
- [117] R. T. ROCKAFELLAR AND R. J. B. WETS, *Variational Analysis*, Springer Berlin Heidelberg, 1998, <https://doi.org/10.1007/978-3-642-02431-3>.
- [118] J. F. RODRIGUES AND L. SANTOS, *Variational and Quasi-Variational Inequalities with Gradient Type Constraints*, Springer International Publishing, 2019, p. 319–361, [https://doi.org/10.1007/978-3-030-33116-0\\_13](https://doi.org/10.1007/978-3-030-33116-0_13).
- [119] F. SANTAMBROGIO, *Optimal Transport for Applied Mathematicians: Calculus of Variations, PDEs, and Modeling*, no. 87 in Progress in Nonlinear Differential Equations and Their Application, Birkhäuser, 2015, <https://doi.org/10.1007/978-3-319-20828-2>.
- [120] O. SAVIN, *Global  $W^{2,p}$  estimates for the Monge–Ampère equation*, Proceedings of the American Mathematical Society, 141 (2013), p. 3573–3578, <https://doi.org/10.1090/s0002-9939-2013-11748-x>.
- [121] T. SCHWEDES, D. A. HAM, S. W. FUNKE, AND M. D. PIGGOTT, *Mesh dependence in PDE-constrained optimisation*, Springer, 2017, <https://doi.org/10.1007/978-3-319-59483-5>.
- [122] J. A. SETHIAN, *A fast marching level set method for monotonically advancing fronts*, Proceedings of the National Academy of Sciences of the United States of America, 93 (1996), pp. 1591–1595, <https://doi.org/10.1073/pnas.93.4.1591>.
- [123] A. SIGNORINI, *Questioni di elasticità non linearizzata e semilinearizzata*, Rendiconti Di Matematica e Delle Sue Applicazioni, 18 (1959), pp. 95–139.
- [124] I. W. STEWART, *The Static and Dynamic Continuum Theory of Liquid Crystals: A Mathematical Introduction*, Liquid Crystals Book Series, Taylor & Francis, 2004.
- [125] T. M. SUROWIEC AND S. W. WALKER, *Optimal control of the Landau–de Gennes model of nematic liquid crystals*, SIAM Journal on Control and Optimization, 61 (2023), pp. 2546–2570, <https://doi.org/10.1137/22m1506158>.
- [126] M. TEBoulLE, *A simplified view of first order methods for optimization*, Mathematical Programming, 170 (2018), p. 67–96, <https://doi.org/10.1007/s10107-018-1284-2>.
- [127] T. W. TING, *Elastic-plastic torsion of convex cylindrical bars*, Journal of Mathematics and Mechanics, 19 (1969), pp. 531–551, <http://www.jstor.org/stable/24901809> (accessed 2024-03-06).
- [128] M. ULBRICH, *Semismooth Newton methods for operator equations in function spaces*, SIAM Journal on Optimization, 13 (2003), pp. 805–841, <https://doi.org/10.1137/S1052623400371569>.
- [129] M. ULBRICH, *Semismooth Newton Methods for Variational Inequalities and Constrained Optimization Problems in Function Spaces*, vol. 11 of MOS-SIAM Series on Optimization, SIAM, 2011, <https://doi.org/10.1137/1.9781611970692>.
- [130] G. M. VASIL, K. J. BURNS, D. LECOANET, S. OLVER, B. P. BROWN, AND J. S. OISHI, *Tensor calculus in polar coordinates using Jacobi polynomials*, Journal of Computational Physics,

- 325 (2016), pp. 53–73, <https://doi.org/10.1016/j.jcp.2016.08.013>.
- [131] A. WÄCHTER AND L. T. BIEGLER, *On the implementation of an interior-point filter line-search algorithm for large-scale nonlinear programming*, Mathematical Programming, 106 (2006), pp. 25–57, <https://doi.org/10.1007/s10107-004-0559-y>.
- [132] W. WANG, L. ZHANG, AND P. ZHANG, *Modelling and computation of liquid crystals*, Acta Numerica, 30 (2021), pp. 765–851, <https://doi.org/10.1017/s0962492921000088>.
- [133] Y. WANG AND J. XU, *Q-tensor gradient flow with quasi-entropy and discretizations preserving physical constraints*, Journal of Scientific Computing, 94 (2022), <https://doi.org/10.1007/s10915-022-02060-x>.
- [134] M. WARBY, J. R. WHITEMAN, W.-G. JIANG, P. WARWICK, AND T. WRIGHT, *Finite element simulation of thermoforming processes for polymer sheets*, Mathematics and computers in simulation, 61 (2003), pp. 209–218, [https://doi.org/10.1016/S0378-4754\(02\)00077-0](https://doi.org/10.1016/S0378-4754(02)00077-0).
- [135] M. WEISER, A. SCHIELA, AND P. DEUFLHARD, *Asymptotic mesh independence of Newton’s method revisited*, SIAM journal on numerical analysis, 42 (2005), pp. 1830–1845, <https://doi.org/10.1137/S0036142903434047>.
- [136] L. W. WHITE, *Control of a hyperbolic problem with pointwise stress constraints*, Journal of Optimization Theory and Applications, 41 (1983), p. 359–369, <https://doi.org/10.1007/bf00935231>.
- [137] W. WOLLNER, *Optimal control of elliptic equations with pointwise constraints on the gradient of the state in nonsmooth polygonal domains*, SIAM Journal on Control and Optimization, 50 (2012), p. 2117–2129, <https://doi.org/10.1137/110836419>.
- [138] K. WU AND C.-W. SHU, *Geometric quasilinearization framework for analysis and design of bound-preserving schemes*, SIAM Review, 65 (2023), pp. 1031–1073, <https://doi.org/10.1137/21M1458247>.
- [139] S. WU AND J. XU, *Multiphase Allen–Cahn and Cahn–Hilliard models and their discretizations with the effect of pairwise surface tensions*, Journal of Computational Physics, 343 (2017), pp. 10–32, <https://doi.org/10.1016/j.jcp.2017.04.039>.
- [140] S. ZAGATTI, *On viscosity solutions of Hamilton–Jacobi equations*, Transactions of the American Mathematical Society, 361 (2009), pp. 41–59, <http://www.jstor.org/stable/40302759>.
- [141] E. ZEIDLER, *Nonlinear Functional Analysis and its Applications: Part 1: Fixed-Point Theorems*, vol. 1 of Nonlinear Functional Analysis and its Applications, Springer, 1986.
- [142] H. ZHAO, *A fast sweeping method for eikonal equations*, Mathematics of Computation, 74 (2004), p. 603–627, <https://doi.org/10.1090/s0025-5718-04-01678-3>.
- [143] H.-K. ZHAO, S. OSHER, B. MERRIMAN, AND M. KANG, *Implicit and nonparametric shape reconstruction from unorganized data using a variational level set method*, Computer Vision and Image Understanding, 80 (2000), p. 295–314, <https://doi.org/10.1006/cviu.2000.0875>.